



# Do Differences in Latitudinal Distributions of Species and Organelle Haplotypes Reflect Thermal Reaction Norms Within the *Emiliana/Gephyrocapsa* Complex?

Peter von Dassow<sup>1,2\*</sup>, Paula Valentina Muñoz Farías<sup>1,3</sup>, Sarah Pinon<sup>2</sup>, Esther Velasco-Senovilla<sup>2,4,5</sup> and Simon Anguita-Salinas<sup>6,7</sup>

<sup>1</sup> Departamento de Ecología, Facultad de Ciencias Biológicas, Pontificia Universidad Católica de Chile, Santiago, Chile, <sup>2</sup> Instituto Milenio de Oceanografía de Chile, Concepción, Chile, <sup>3</sup> Fundación Mujeres de Mar, Viña del Mar, Chile, <sup>4</sup> Centro Oceanográfico de Vigo, Instituto Español de Oceanografía (IEO-CSIC), Vigo, Spain, <sup>5</sup> Facultad de Ciencias del Mar, Universidad de Vigo, Vigo, Spain, <sup>6</sup> Departamento de Zoología, Facultad de Ciencias Naturales y Oceanográficas, Universidad de Concepción, Concepción, Chile, <sup>7</sup> Instituto de Ecología y Biodiversidad, Santiago, Chile

## OPEN ACCESS

### Edited by:

Gustavo Fonseca,  
Federal University of São Paulo, Brazil

### Reviewed by:

Marco C. Brustolin,  
Norwegian Institute of Marine  
Research (IMR), Norway  
Matthew Lee,  
Universidad de Los Lagos, Chile

### \*Correspondence:

Peter von Dassow  
pvondassow@bio.puc.cl

### Specialty section:

This article was submitted to  
Marine Evolutionary Biology,  
Biogeography and Species Diversity,  
a section of the journal  
Frontiers in Marine Science

**Received:** 29 September 2021

**Accepted:** 28 October 2021

**Published:** 02 December 2021

### Citation:

von Dassow P, Muñoz Farías PV,  
Pinon S, Velasco-Senovilla E and  
Anguita-Salinas S (2021) Do  
Differences in Latitudinal Distributions  
of Species and Organelle Haplotypes  
Reflect Thermal Reaction Norms  
Within the *Emiliana/Gephyrocapsa*  
Complex? *Front. Mar. Sci.* 8:785763.  
doi: 10.3389/fmars.2021.785763

The cosmopolitan phytoplankter *Emiliana huxleyi* contrasts with its closest relatives that are restricted to narrower latitudinal bands, making it interesting for exploring how alternative outcomes in phytoplankton range distributions arise. Mitochondrial and chloroplast haplogroups within *E. huxleyi* are shared with their closest relatives: Some *E. huxleyi* share organelle haplogroups with *Gephyrocapsa parvula* and *G. ericsonii* which inhabit lower latitudes, while other *E. huxleyi* share organelle haplogroups with *G. muelleriae*, which inhabit high latitudes. We investigated whether the phylogeny of *E. huxleyi* organelles reflects environmental gradients, focusing on the Southeast Pacific where the different haplogroups and species co-occur. There was a high congruence between mitochondrial and chloroplast haplogroups within *E. huxleyi*. Haplogroup II of *E. huxleyi* is negatively associated with cooler less saline waters, compared to haplogroup I, both when analyzed globally and across temporal variability at the small special scale of a center of coastal upwelling at 30° S. A new mitochondrial haplogroup Ib detected in coastal Chile was associated with warmer waters. In an experiment focused on inter-species comparisons, laboratory-determined thermal reaction norms were consistent with latitudinal/thermal distributions of species, with *G. oceanica* exhibiting warm thermal optima and tolerance and *G. muelleriae* exhibiting cooler thermal optima and tolerances. *Emiliana huxleyi* haplogroups I and II tended to exhibit a wider thermal niche compared to the other *Gephyrocapsa*, but no differences among haplogroups within *E. huxleyi* were found. A second experiment, controlling for local adaptation and time in culture, found a significant difference between *E. huxleyi* haplogroups. The difference between I and II was of the expected sign, but not the difference between I and Ib. The differences were small ( $\leq 1^{\circ}\text{C}$ ) compared to differences reported previously within *E. huxleyi* by local adaptation and even in-culture evolution. Haplogroup Ib showed a narrower thermal niche. The cosmopolitanism of *E. huxleyi*

might result from both wide-spread generalist phenotypes and specialist phenotypes, as well as a capacity for local adaptation. Thermal reaction norm differences can well explain the species distributions but poorly explain distributions among mitochondrial haplogroups within *E. huxleyi*. Perhaps organelle haplogroup distributions reflect historical rather than selective processes.

**Keywords:** *Emiliana huxleyi*, *Gephyrocapsa*, phytoplankton, thermal reaction norms, thermal performance curves, haplogroup, cytochrome oxidase

## INTRODUCTION

Rising atmospheric CO<sub>2</sub> is driving rapid changes in the ocean, including ocean acidification, increased stratification, and an increase in average surface temperature (Hoegh-Guldberg and Bruno, 2010; Gattuso et al., 2015; Pörtner et al., 2019). Temperature is a key factor in determining the productivity (Laws et al., 2000) as well as the biochemical and elemental composition of marine phytoplankton (Toseland et al., 2013), microorganisms responsible for roughly half of global photosynthesis (Field et al., 1998). Likewise, temperature is frequently identified as a key variable related to differences in community composition. At a global scale, phytoplankton exhibit thermal optima for growth that vary with habitat temperature (Thomas et al., 2012). It has been postulated that there should be trade-offs limiting the ability to adapt to a wide range of temperatures. First, adaptation to higher temperature decreases performance at lower temperature, and vice versa (Norberg, 2004). Second, a generalist-vs-specialist trade-off is expected, where an increasing width of the thermal reaction norm (niche width) may come at the cost of reduced maximal performance under optimal conditions (Izem and Kingsolver, 2005). Thus, temperature is expected to be an important determinant in the distributions of phytoplankton species and perhaps genotypes within species.

However, thermal widths for growth in phytoplankton are quite broad in comparison to their oceanographic distributions (Thomas et al., 2012; Boyd et al., 2013; Anderson and Rynearson, 2020). In fact, in those studies the upper thermal limits and even optima for growth in the lab can far exceed temperatures experienced in the environment from which organisms are isolated. Further, it has been difficult to measure thermal niche width in phytoplankton (Boyd et al., 2013), so a generalist-vs-specialist trade-off in phytoplankton has not been demonstrated. Finally, in the lab, selection can shift thermal optima of marine phytoplankton in only a few hundred asexual generations (Listmann et al., 2016; O'Donnell et al., 2018).

The eukaryotic phytoplankton *Emiliana huxleyi* is exceptional in the breadth of its distribution, being the dominant or co-dominant member of its functional group, coccolithophores, in most of the global surface ocean, from the tropics to the sub-polar (and now even polar) regions, and from highly productive coastal and estuarine environments to the oligotrophic central gyres (Paasche, 2001; Winter et al., 2014). The taxon appeared in the fossil record only 291000 years ago (Raffi et al., 2006), and became a globally dominant coccolithophore within the last 100000 years with fluctuations in its relative abundance

associated with global climate shifts (Bendif et al., 2019). Despite high morphological (Young and Westbroek, 1991), physiological (Meyer and Riebesell, 2015; Feng et al., 2017; Echeveste et al., 2018), and even genome content variability (Read et al., 2013; von Dassow et al., 2015) among *E. huxleyi* strains, phylogenomic analysis suggested that the recent evolution of *E. huxleyi* is as a single species (Filatov, 2019). In addition, this species is comparatively easy to isolate and maintain in culture, and isolates seem to reflect natural populations in terms of morphotypes (von Dassow et al., 2018) and possibly in genetic markers as well (Beaufort et al., 2011).

At the LSU and SSU rRNA genes, markers classically used at species-level identification, *E. huxleyi* is identical or nearly identical to close relatives taxonomically classed in the genus *Gephyrocapsa*, distinguished morphologically from *E. huxleyi* principally by the presence of a bridge over the coccolith central area in most *Gephyrocapsa* (with the exception of those previously classified as *Reticulofenestra*) (Medlin et al., 1996; Young et al., 2003; Bendif et al., 2016). Based on organellar and nuclear 18S and 28S single gene phylogenies, and on phylogenomics analysis, *Emiliana* and *Gephyrocapsa* should more appropriately be considered as congeners (Bendif et al., 2016, 2019), however we retain the traditional taxonomic genus name *Emiliana* here awaiting formal re-assignment. The mitochondrial cytochrome oxidase (*cox*) genes consistently separate *E. huxleyi* from *G. oceanica* (Hagino et al., 2011; Bendif et al., 2014). However, *E. huxleyi* contains two mitochondrial haplogroups based on cytochrome oxidase (*cox*) genes, of which Haplogroup I (also called alpha) is shared with the species *G. ericsonii* and *G. parvula* (which are not separated by organelle or nuclear phylogenetic markers or phylogenomics), while the Haplogroup II (also called beta) is shared with *G. muelleriae* (Bendif et al., 2016).

Curiously, the broad, apparently generalist, distribution of *E. huxleyi* is contrasted with the much narrower latitudinal distributions of its closest relatives which appear to occupy narrower niches. *G. oceanica* appears to be roughly restricted to temperatures above about 15°C in the Atlantic and 19°C in the Pacific (McIntyre et al., 1970; Okada and McIntyre, 1977; Bollmann, 1997; Bollmann and Klaas, 2008; Beaufort et al., 2011), and corresponds to Haplogroup III (Hagino et al., 2011). Both *G. ericsonii* and *G. parvula* (formerly *Reticulofenestra parvula*) represent the smallest members of the genus and appear to be associated with sub-tropical and tropical waters, whereas, in contrast, *G. muelleriae* is restricted to cooler waters below 21°C (McIntyre et al., 1970; Okada and McIntyre, 1977; Bollmann, 1997; Bollmann and

Klaas, 2008; Bendif et al., 2016). *Emiliania huxleyi* which share Haplogroup I with *G. ericsonii/parvula* exhibit a lower latitude, warm-water distribution, while *E. huxleyi* which share Haplogroup II with *G. muelleriae* exhibited a higher latitude, cool-water distribution (Hagino et al., 2011; Bendif et al., 2016). Latitudinal gradients in mitochondrial haplotypes are common in animals including humans (Mishmar et al., 2003; Camus et al., 2017) and the mitochondrial genome was reported to impact thermal tolerance by on the order of 5°C in yeast in crosses of closely related cold-tolerant and warm-tolerant species (Baker et al., 2019). Thus, the principal genetic separation within *E. huxleyi*, which might represent introgression among closely related species or incomplete lineage sorting from a common ancestor, corresponds to an ecological separation along latitudinal gradients implying a role for temperature. This makes the *Emiliania/Gephyrocapsa* group particularly interesting for exploring how temperature affects both species and genotype distributions.

Previous studies have suggested that *E. huxleyi* exhibits thermal adaptations to its local habitat. An influential study published almost four decades ago reported that the ratio of growth rates at 26° to 16° was lower for five strains from the Gulf of Maine compared to 68 strains from the Sargasso Sea (Brand, 1982). A study reported that two strains from high latitudes grew at 6°C but not 27°C, while one strain from low latitude grew at 27°C but not 6°C (Conte et al., 1998). More recently, comparison of six sub-tropical central Atlantic (Azores) isolates and five sub-polar isolates from Bergen revealed that Bergen isolates could grow faster at 8°C, while central Atlantic (Azores) isolates could grow at 28°C, a temperature which did not permit growth of Bergen isolates, and the thermal optima averaged 1°C higher in Azores isolates (Zhang et al., 2014). Meanwhile, in asexually reproducing populations originating from the same original clone, the optimum growth temperature was reported to change by 0.7°C and the maximum persistence temperature to change by nearly 2°C after growth in the lab at 26.3 vs. 15°C for 1200 generations, which was interpreted to reflect in-culture adaptive evolution (Listmann et al., 2016). That is, a few hundred generations of asexual growth could produce nearly the same thermal performance differences as seen over the thousands of km between Bergen and the Azores.

Here we focused on testing the latitudinal distributions and thermal habitats of mitochondrial haplogroups on the regional scale. We chose the Southeast Pacific. The *G. ericsonii/parvula* group, which shares the *cox* haplogroup I, occurs with *E. huxleyi* in the warmer northern waters of this zone, while *G. muelleriae*, which shares the *cox* haplogroup II, is found in the south-central Chilean upwelling zone (Bendif et al., 2016; von Dassow et al., 2018), and *E. huxleyi* of both haplogroups co-exist to the west of central Chile (Beaufort et al., 2011). Previous studies have also documented incongruence of mitochondrial phylogenies and chloroplast phylogenies (e.g., based on *tufA*) (Bendif et al., 2014, 2016). If mitochondrial and chloroplast histories are very distinct, this would need to be taken into account in interpretations of environmental patterns and experimental design, as well as having implications for the recent evolutionary diversification of

*E. huxleyi*. A total of 407 strains from this region were isolated and genotyped for *cox* haplogroup, of which 161 were also genotyped for *tufA* haplotype.

We also experimentally tested the following specific hypotheses, aiming to control for possible effects of local adaptation and in-culture evolution in one set of tests focused on within-species comparisons:

1. Inter-specific differences in thermal reaction norms among species in the *Emiliania-Gephyrocapsa* genus account for latitudinal range distributions.
2. Intra-specific differences in the thermal reaction norms between the two *E. huxleyi* mitochondrial haplogroups account for their latitudinal range distributions. The broader latitudinal distribution of *E. huxleyi* reflects either.
3. A thermal niche that is wider than closely related species of narrower latitudinal distributions, or, alternatively,
4. Different genotypes that have similar niche widths that are shifted to warmer or cooler temperatures by phylogenetic history and/or thermal adaptation.

## MATERIALS AND METHODS

### Strain Origins and Field Sampling

Isolation of strains from coastal Chile, the Juan Fernandez Archipelago, and oceanic waters west of Peru between 2011 and 2013 was previously described (Bendif et al., 2016; von Dassow et al., 2018). In November-December 2015, strains were isolated from 3 stations during the LowpHOx 1 cruise aboard the R/V Cabo de Hornos. To be able to compare to previous strains collected from near the Punta Lengua de Vaca upwelling at 30°S, water was collected from the onboard continuous seawater system as the ship passed this latitude, and temperature and salinity were recorded from the ships thermosalinometer. At two other stations, water was sampled from 5 m from the CTD rosette equipped with 10L Niskin bottles. In August 2016 a one-day field campaign was conducted on the R/V Stella Maris II from Coquimbo to south of Punta Lengua de Vaca, and water was collected from beside the boat using a torpedo system connected to a CTD pump as previously described. Following previously described protocols, water samples (100 ml) were concentrated to 1–2 ml by gentle centrifugation and coccolith-bearing cells were individually isolated based on depolarization of forward scatter light by an InFlux Mariner Cell Sorter flow cytometer (von Dassow et al., 2012, 2018; Bendif et al., 2016). In the LowpHOx 1 cruise, the flow cytometer was onboard and samples were processed immediately. In 2016, samples were carried in coolers to the lab in Santiago for processing the next day. Details of strain origins are provided in **Supplementary File 1**.

Once established, strains were identified by scanning electron microscopy (SEM) to species-level (*E. huxleyi* or *Gephyrocapsa* species) and morphotype (*E. huxleyi*) and classified (von Dassow et al., 2018). Strains were then maintained in L1 medium in an environmental chamber on a 12:12 light-dark cycle

where temperature fluctuated from 14 (lights off) to 15°C (lights on). Cultures were maintained by transfer to fresh medium every 3–4 weeks.

## Partial Sequencing and Analysis of *cox1*, *cox3*, and *tufA* Genes

Cultures were collected by filtration or centrifugation and DNA was extracted using either a DNeasy Plant Mini kit (Qiagen) or following a modified CTAB protocol: Cells pelleted by centrifugation were extracted in 700  $\mu$ l of 100 mM Tris-HCl (pH 7.5), 25 mM EDTA, 1.5 M NaCl, 2% (w/v) CTAB, and 0.3% (v/v)  $\beta$ -mercaptoethanol, ground with acid-washed glass beads, and 3  $\mu$ l of proteinase K (20 mg ml<sup>-1</sup>) was added. Subsequent steps followed a protocol for recalcitrant plants (Healey et al., 2014). PCR and partial sequencing of *cox1*, *cox3*, and *tufA* were performed as described previously (Bendif et al., 2016). Additionally, partial *cox1* and *cox3* sequences were downloaded from Genbank and those that could be aligned over sections of 1375 (*cox1*) or 810 bp (*cox3*) were kept for analysis. Sequences were aligned with ClustalW. Haplotype networks were constructed individually for all three markers, as well as on the concatenated *cox1-cox3* alignment, by median joining (Bandelt et al., 1999) using PopART (Leigh and Bryant, 2015). Genetic groups were determined for all three alignments using Automatic Barcode Gap Discovery (ABGD) (Puillandre et al., 2012). Gene trees were constructed using Maximum Likelihood using RaxMLGUI 2.0 (Bootstrap = 1000, GTR+I+G) on CIPRES, and in parallel with Bayesian Inference on Mr. Bayes (HKY+I+G, 50M of generations, sample frequency every 1000, temperature 0.30, burning 25%).

## Characterizing Environments of Origins of Strains

For most strains for which *cox1* and/or *cox3* sequences are available in Genbank, location and month of isolation, but not associated environmental data, is available as meta-data either from the source literature or from public data provided by culture collections (see **Supplementary Files 1, 2**). Reconstructed ocean environmental parameters sea surface temperature (SST), sea surface salinity (SSS) and mixed layer depth (MLD) was assigned to all strains isolated after 1993 (from which *cox1* and/or *cox3* sequences were used here) using the Multi Observation Global Ocean ARMOR3D L4 analysis and multi-year reprocessing (Guinehut et al., 2012; Mulet et al., 2012) actualized from the Copernicus Marine Services website<sup>1</sup> on 20 Feb 2020. Minimum distance to mainland coast of strain origins was estimated using Google Earth. In that analysis, the mainland coast was the nearest continent or coast of large islands (>100,000 km<sup>2</sup>, e.g., Iceland or Japan). For each strain origin location and date, the monthly mean SST, SSS, and MLD was extracted. Multinomial logistic regression was performed using the *nnet* package (Ripley and Venebles, 2021) in R (R Core Team, 2020). For strains isolated from the Southeast Pacific by the lead author or lab members for which direct measurements of SST and SSS are available

(**Supplementary File 2**), an additional analysis was performed using these data.

## Experiments to Determine Temperature-Dependence of Growth Rate

### Experiment 1 to Test Differences Among Species (Hypotheses 1 and 3)

These experiments were begun in July 2015. Growth experiments were conducted at 8, 12, 15, 18, 21, 24, 27, and 30°C in transparent tanks filled with water maintained at specified temperatures through a recirculating chiller (SunSun HYH-0.25D-D), coupled with an aquarium heater for higher temperatures. To allow physiological acclimation but minimize the possibility of in-culture evolution, strains were first acclimated to each temperature condition for a minimum of two transfers to fresh medium (corresponding to a minimum of 7 asexual generations). Additionally, to minimize thermal shocks, acclimation was progressive to temperatures above 18°C or below 15°C. That is, strains would be acclimated to a new temperature (further from their temperature of maintenance) only after acclimating to the previous temperature. For example, strains tested at 27°C were first acclimated at 24°C. This means, for example, that strains which grew poorly or not at all at 24°C were not tested at higher temperatures. Light was maintained at 150  $\mu$ mol phot m<sup>-2</sup> s<sup>-1</sup> by cool-white fluorescent tubes. Acclimation and experimental cultures were in sealed 5 ml transparent polystyrene culture tubes (Falcon 352003, Corning). Fluorescence was read directly in the culture tubes with an AquaFluor fluorometer (Turner), a strategy commonly used in such studies to avoid opening and sampling repeatedly for counting (Brand et al., 1981; Brand, 1982; Anderson and Rynearson, 2020). Initial experiments showed that patterns of growth at different temperatures were similar in tubes and in larger 50 ml experimental cultures in flasks, and also that fluorescence tracked cell abundance counted with a Neubauer haemocytometer in acclimated cultures before cultures entered stationary phase (data not shown). After the first acclimation culture, acclimation and experimental cultures were inoculated from cultures that were in active, near exponential growth (fluorescence <20% of maximum yield, corresponding to cell abundances of <2  $\times$  10<sup>5</sup> ml<sup>-1</sup> for the smallest species), and exponential growth rate was measured only from points where fluorescence was <10% of typical final growth yield. When cultures failed to acclimate to a new temperature, growth rate at that temperature was recorded as 0 as negative growth rates could not be confidently measured with this approach.

Because of the dearth of strains (in any culture collection) for some haplogroups and species, Experiment 1 had an unbalanced study design among *E. huxleyi* haplogroups and closely related species: There were six strains of *E. huxleyi* haplogroup I, four of *E. huxleyi* haplogroup II, five of *G. parvula/ericsonii* (considered con-specifics by single gene phylogenies as well as phylogenomics, so grouped here; see Bendif et al., 2016, 2019), three of *G. muelleriae*, and six of *G. oceanica* (**Table 1**). All *E. huxleyi* strains were obtained from

<sup>1</sup><https://marine.copernicus.eu/>

the original SEPA collection<sup>2</sup>, while the clonal duplicates of some *G. parvula/ericsonii* and *G. muelleriae* strains were obtained from the Roscoff Culture Collection (RCC<sup>3</sup>). One of the three original *G. muelleriae* strains to be isolated (Bendif et al., 2015) did not survive transport from the RCC back to Chile, so when we realized that we had isolated a new *G. muelleriae* strain from the LowpHOx I cruise, this strain was included in Experiment 1, to have three strains of this species to permit statistical tests among species. Originally, six strains of haplogroup I and six of haplogroup II were selected arbitrarily, but adequate data to evaluate growth at 27°C were not obtained from two strains of haplogroup II despite max. growth at 24°C, meaning that thermal performance curves were fit for only four haplogroup II strains. The single strain of haplogroup Ib isolated before 2015 (SEPA118) was also analyzed, to allow qualitative comparison, but results from that single strain were excluded from statistical tests in Experiment 1. To our knowledge, the only *G. muelleriae* and *G. parvula/ericsonii* strains currently available in culture collections all come from the Chilean coast, but *G. oceanica* isolates from this region were not available, so six *G. oceanica* strains from different global origins were obtained from the RCC. As all *G. oceanica* survived transport to Chile, all were included.

### Experiment 2 to Test Differences Among Haplogroups Within *E. huxleyi* Species (Hypotheses 2, 3, and 4)

We originally aimed to include seven strains of *E. huxleyi* isolated from the LowpHOx I cruise in each genetic group in order to have at least a similar power to discriminate differences among genetic groups as the ability by Zhang et al. (2014) to distinguish differences among geographic locations. However, since we also aimed to complete growth experiments within 18 months after initial isolation (to minimize in-culture evolution), it was necessary to begin experiments before genetic data was complete. Therefore we arbitrarily selected 15 strains in March 2016, once cultures had been established. When first molecular and SEM data became available, a further 12 strains of *E. huxleyi* were added in July 2016 to make a larger total of 27 strains. 25 of these strains come from the same water sample at 27° S. To ensure that we would have the chance to compare an adequate number of haplogroup II strains when genetic data was not complete, 2 strains were arbitrarily selected also from the site at 30° S where this haplogroup was dominant in previous samplings. As we initiated growth acclimations before having completed analysis of genetic data, the groups are not of the same size: 8 were in mitochondrial haplogroup I, 9 in haplogroup II, and 10 in the newly observed (see below) haplogroup Ib (Table 1).

### Analysis of Thermal Reaction Norms

Thermal reaction norms here are based on fitting Thermal Performance Curves (TPCs) for growth. Two parallel TPC analyses were performed. Recent comparative work analyzing or re-analyzing published TPC data in diverse phytoplankton (Thomas et al., 2012; Boyd et al., 2013; Anderson and Rynearson, 2020) have fit such data to the Norberg equation (Norberg,

2004), a general function for a temperature response for growth based on the Eppley curve, an envelope function proposed to describe an evolutionary limit to maximum growth rate vs. temperature (Eppley, 1972). Such an approach has also been used for investigating asexual evolution of thermal reaction norms in clonal populations of *E. huxleyi* subject to selection in the lab at different temperatures (Listmann et al., 2016). For comparison with this literature base, it is our primary analysis. The general Norberg equation gives growth rate  $\mu_i$  as a function of temperature  $T$  for individual or species  $i$  as:

$$\mu_i(T) = a_i e^{bT} \left[ 1 - \left( \frac{T - Z_i}{W_i/2} \right)^2 \right] \quad (1)$$

where the trait  $Z_i$  is the temperature at which growth approaches the Eppley curve optimum, and  $W_i$  is the thermal niche width (in °C). Thus  $Z_i$  is not the temperature of maximal growth but the temperature at which maximal growth is closest to the maximum exhibited by phytoplankton generally at that temperature, a represents a competitive optimum. Norberg's derivation fixed the Eppley curve coefficient  $a$  at 0.59 and the exponent  $b$  at 0.0633 (Norberg, 2004). Both  $a$  and  $b$  have been considered by other authors to be free parameters to fit in published analysis of experimental TPC curves (Thomas et al., 2012; Boyd et al., 2013; Listmann et al., 2016). We returned to the original interpretations of Norberg and Eppley (Eppley, 1972; Norberg, 2004), that the envelope represents a constant shape defining the observed upper limits of phytoplankton performance with temperature across all species, and kept  $b$  fixed at 0.0633 while letting  $a_i$  vary among strains. In this way,  $a_i$  has a simple biological interpretation:  $a_i/0.59$  is the degree to which strain  $i$  reaches the envelope maximum at  $T = Z_i$ . In fact, for many strains it was not possible to obtain adequate fits, or reasonable values of  $Z_i$ , when  $b$  was free. Also, Thomas et al. (2012) used  $b = 0.0631$  as a theoretical value, but we found slightly better fits keeping  $b = 0.0633$  (not shown). Curve fitting for the Norberg equation was performed in Prism 9 (GraphPad Software). We note that previous studies have derived  $T_{opt,i}$ , the temperature of maximum growth, from the Norberg equation and reported this. We were interested in comparing the both thermal niche width  $W_i$  and  $T_{opt,i}$ .  $T_{opt,i}$  was derived numerically in R from both both  $Z_i$  and  $W_i$ , so is not independent, and only  $Z_i$  and  $W_i$  were used for statistical testing.

A key previous study on *E. huxleyi* thermal reaction norms (Zhang et al., 2014) instead used the Template Mode of Variation (TMV) approach, so we also performed TMV analysis in order to compare differences among groups most directly to what was observed in that study. The TMV approach also has the advantage of accommodating more complex TPC shapes (Izem and Kingsolver, 2005). This involves finding a common curve shape  $f(x)$  to the individuals to be compared, and then for each individual  $i$  an individual curve is fitted:

$$\mu_i(T) = \frac{1}{w_i} f\left(\frac{T - m_i}{w_i}\right) + h_i \quad (2)$$

Here,  $m_i$  is the temperature of maximal growth (from here on referred to as  $T_{opt}$ ),  $h_i$  is the height parameter (average growth rate), and  $w_i$  is the non-dimensional width parameter.

<sup>2</sup><http://sepa.bio.puc.cl/>

<sup>3</sup><http://roscoff-culture-collection.org/>

Here a polynomial of degree 4 was fit for  $f(x)$ , following Zhang et al. (2014). The fit was performed in Matlab using the scripts provided by Izem and Kingsolver (2005). A large number of strains (most *E. huxleyi*, all *G. oceanica*, and most *G. parvula*) grew positively at 27°C and it was necessary to include this point to ensure a value of  $\mu_i(T)$  at a temperature higher than the temperature of maximum growth, while no *G. muelleriae* grew at 24°C and so could not be tested at 27°C using the progressive acclimation approach. The TMV scripts require at least one data point at all temperatures tested, so *G. muelleriae* had to be analyzed separately. By visual inspection, we detected isolated cases where the TMV analysis appeared to strongly overestimate max growth rate (and therefore the height parameter  $h_i$ ) compared to the Norberg curve fits. This might relate in part to the fact that we could not measure negative growth rates. The empirical minimum growth rate was constrained at 0 but the fit polynomial in TMV analysis could go below 0, which would affect the weighted sum-of-squares error in the fitting procedure. Therefore, we used the TMV analysis only to compare differences in  $T_{opt}$  observed here to those reported by Zhang et al. (2014).

### Statistical Analyses of Differences Inter- and Intraspecific Differences in Thermal Reaction Norms

For *E. huxleyi* haplogroups I and II in the first experiment and all groups of *E. huxleyi* strains in the second experiment, the

number of strains was sufficient to allow normality testing. The distributions of  $a$ ,  $Z$  and  $W$  from the Norberg fits and the  $w$ ,  $h$ , and  $T_{opt}$  from TMV fit were all consistent with normality according to the Kolmogorov-Smirnov and Shapiro-Wilk tests. For these parameters, significance of differences among groups was evaluated using 1-way ANOVA tests with Tukey's multiple comparison test to identify significant pairwise differences. The distribution of  $w$  from TMV fits did not pass normality tests for *E. huxleyi* haplogroup I from either experiment, so this parameter was compared using the Kruskal-Wallis test with Dunn's test for determining significances of pairwise differences. These tests were performed in Prism 9 (GraphPad Software).

## RESULTS

### Network Analysis Identifies Principal *cox* Haplogroups: New Sub-Group Ib in the Southeast Pacific

A haplotype network was constructed for the concatenated *cox1-cox3* alignments of 186 strains for which both mitochondrial markers were available (Figure 1), a number which includes 163 strains newly sequenced here (119 new strains from 2015 and 2016 campaigns, 44 strains isolated by the same methods between 2011 and 2013), and 23 sequences from Genbank. ABGD analysis supported three or four separate

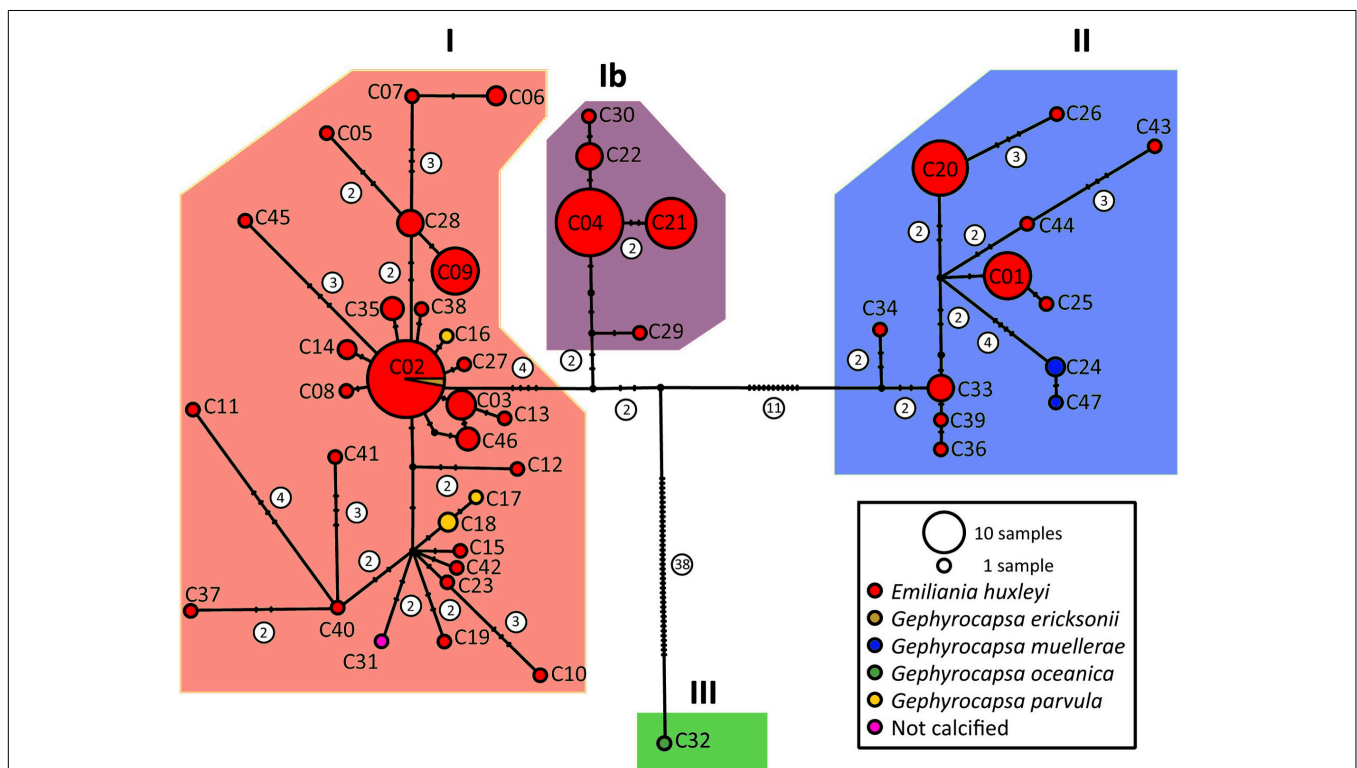


**FIGURE 1 |** Haplotype network based on concatenated alignment of *cox1-cox3*. Diagnostic graphs for the ABGD analysis are in **Supplementary Figure 1**. The same network is re-plotted with key strains in **Supplementary Figure 2**, haplogroups are given in **Supplementary Figure 3** and **Supplementary File 1**. The latter file also associates strains and haplotypes. ABGD analysis and haplotype networks for *cox1* and *cox3* separately are in **Supplementary Figures 4-9**.

haplogroups (see **Supplementary Figures 1–3**). The three group separations corresponded to the clades I, II and III previously defined (Hagino et al., 2011; Bendif et al., 2014, 2016; although termed  $\alpha$ ,  $\beta$  and  $\gamma$ , respectively, in the latter two studies, we revert to the roman numeral designation to avoid confusion with morphotype classifications A, B, and C, and adopt the term haplogroup). No haplogroup III (*G. oceanica*) strains were isolated by this study in the Southeast Pacific, but both haplogroups previously documented for *E. huxleyi* were present. However, with the four group separation proposed by ABGD, clade I was separated into two haplogroups, with haplogroup Ib composed only of strains isolated from the Southeast Pacific. Both Maximum Likelihood and Bayesian trees (**Figure 2**) agreed with the placement of haplogroup Ib as basal to haplogroup I, but with only moderate support (77% bootstrap support and 75% posterior probability).

Sequences were available only for the shorter *cox3* from 324 strains, while only *cox1* was available for 17 strains in Genbank and 3 strains sequenced here. To extend the study to include these 344 strains, haplotype networks for *cox1* and *cox3* were analyzed separately (**Supplementary Figures 4–9**). ABGD analysis assigned the four *G. oceanica* strains for which *cox1* sequences were available (clade III) to two distinct haplogroups. More importantly, *cox1* and *cox3* haplotype networks were

congruent in the assignment into haplogroup I composed of *G. parvula*, and *G. ericsonii*, and some strains of *E. huxleyi*, and haplogroup II composed of *G. muelleriae* and the other strains of *E. huxleyi*. Additionally, although ABGD analysis did not provide support for separating haplogroup Ib from I based on the shorter *cox1* or *cox3* sequences alone, strains could be assigned to *cox1–cox3* haplogroup Ib based on the haplotypes assigned from networks built with either *cox1* or *cox3* separately, so there was no evidence for haplogroup 1b outside of the 412 strains from the Southeast Pacific.

### Tight Association Between Mitochondrial and Chloroplast Haplogroups

A *tufA* haplotype network was constructed from the alignment of 172 total sequences, including 161 sequences from our Southeast Pacific isolates and 11 sequences that could be included in the alignment that were obtained from Genbank from other strains. The *tufA* network was divided into 4 groups by ABGD analysis (**Figure 3** and **Supplementary Figures 10–12**). One group was populated by sequences from only two *E. huxleyi* strains from the Southeast (SEPA25 and SEPA584) and another group by a single sequence of *G. oceanica* (RCC1316). Within the strains from the Southeast Pacific, there was a very strong association

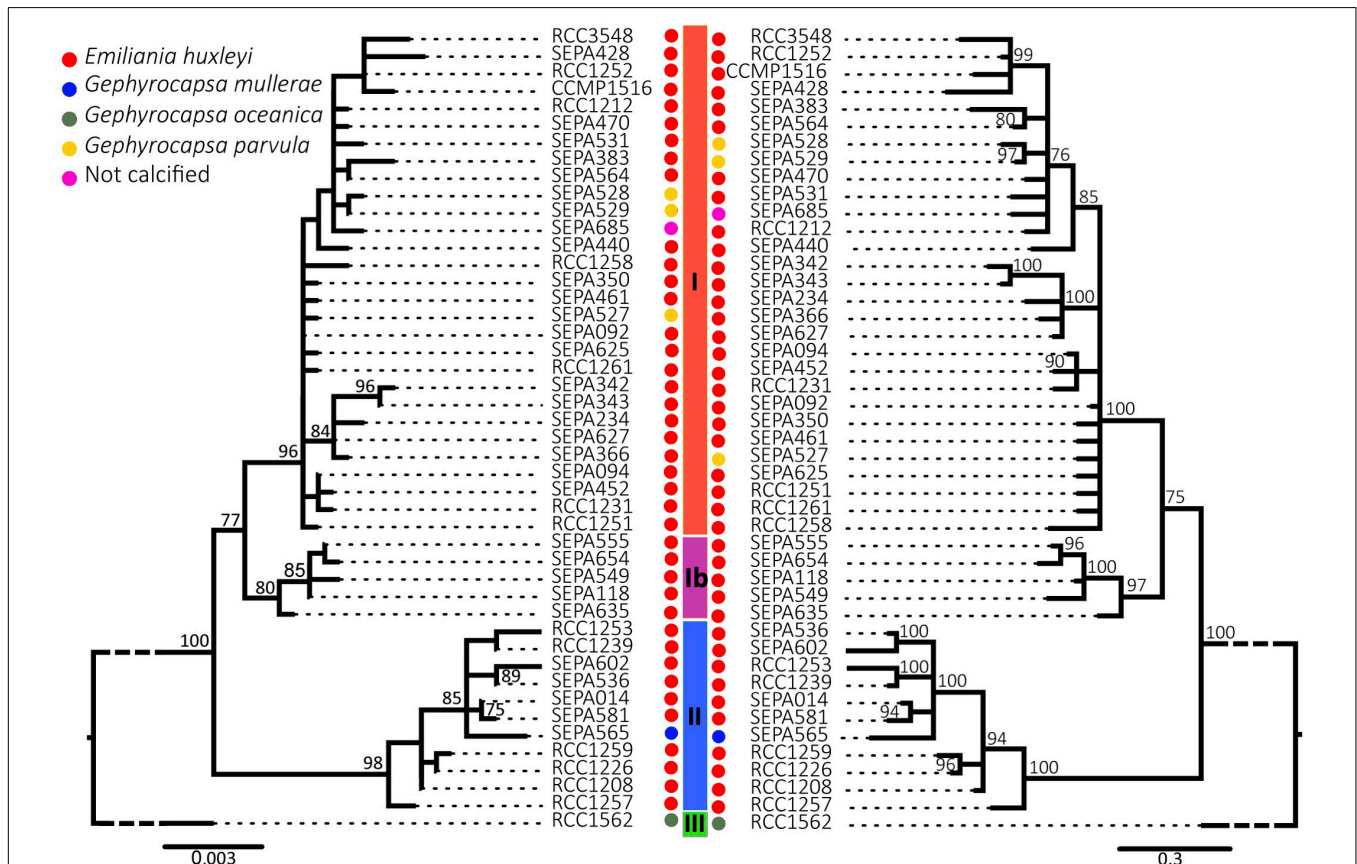
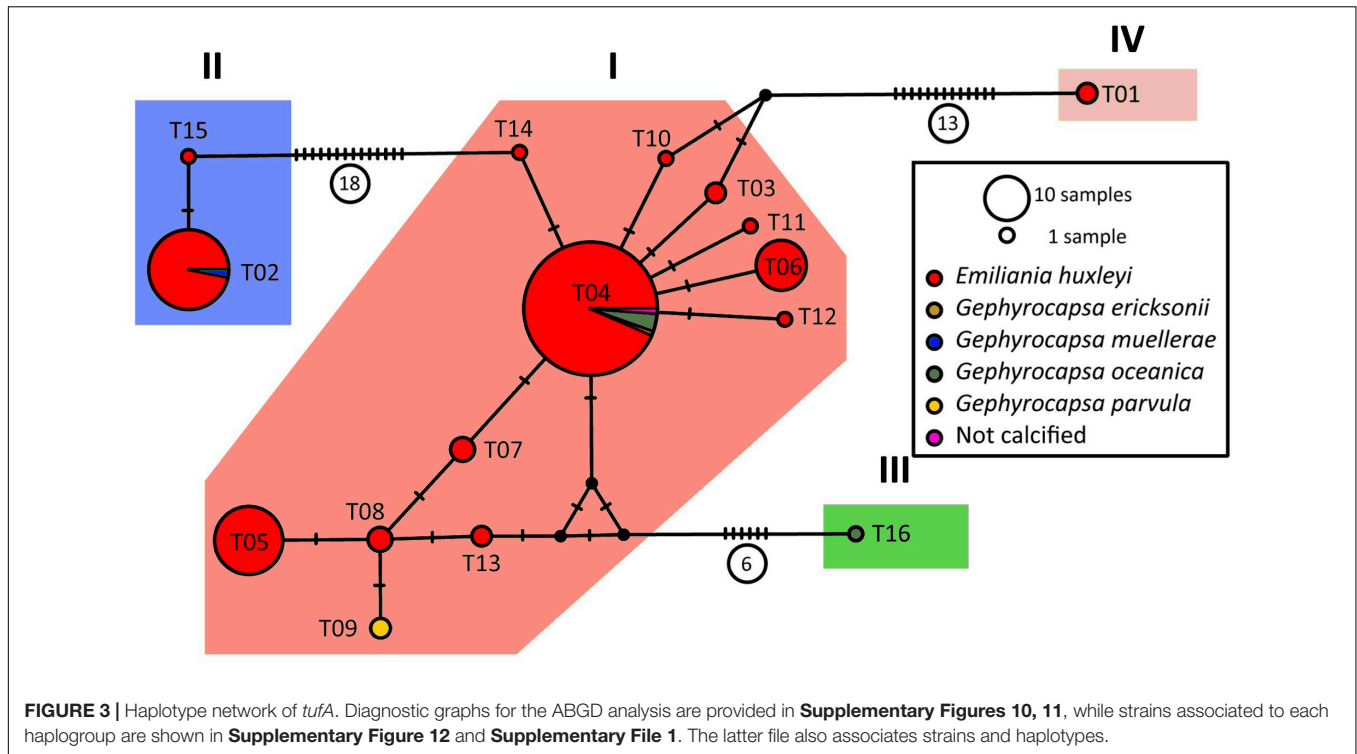


**FIGURE 2 |** Phylogenetic tree of constructed from concatenated *cox1–cox3* alignment. At nodes are shown bootstrap (Maximum Likelihood, left tree) or posterior probability support (Bayesian Inference, right tree) values above 75%.



between mitochondrial and chloroplast haplogroups ( $c^2 = 184.8$ ,  $df = 4$ ,  $p < 0.0001$ ) (Table 2). Only a single *cox* haplogroup Ib isolate was assigned to *tufA* haplogroup II rather than I (of 48 sequenced for both mitochondrial and chloroplast markers), only a single *cox* haplogroup II isolate was assigned to *tufA* haplogroup I (out of 29). Thus, for the rest of the analysis we focus only on *cox* haplogroups.

### Imperfect Association Between Morphotypes and Mitochondrial Haplogroup

Morphological classification was obtained or previously available for a total of 181 strains isolated from the Southeast Pacific between 2011 and 2015. Examples of each morphotype from 2015 to 2016 are shown in **Supplementary Figure 13** and

morphological analysis identifying SEPA565 as a new isolate of *G. muelleriae* by comparison to Bendif et al. (2015, 2016) is provided in **Supplementary Table 1**. There was a significant difference among haplogroups in the distribution of morphotypes ( $c^2 = 135.5$ ,  $df = 2$ ,  $p < 0.0001$ ) (Table 3). Substantial numbers of all three haplogroups were in the broad B morphotype class, which here may include B, B/C, and O morphotypes that were not distinguished here. Almost all of the haplogroup Ib strains were B morphotype. The A-OC morphotype included substantial numbers of both haplogroups I than II. The two morphotypes with over or hypercalcification (closed central area or fusion of distal shield elements) showed contrasting distributions among haplogroups: The A-CC morphotype, with closed central area but separated distal shield elements, was almost exclusively haplogroup I, while the HC/R morphotype (with fused distal shield elements) was almost exclusively haplogroup II. Nevertheless, there was no case where a morphotype was exclusively populated by one mitochondrial haplogroup.

**TABLE 1 |** Numbers of strains of each species or haplogroup used in each experiment.

Species	Haplogroup	Exp. 1	Exp. 2
<i>E. hux.</i>	I	6	8
	Ib	1	10
	II	4	9
<i>G. eric.</i>	I	1	n/a
<i>G. parv.</i>	I	4	n/a
<i>G. muel.</i>	II	3	n/a
<i>G. oce.</i>	III	6	n/a

Strains used and thermal reaction norms calculated are listed in **Supplementary File 4**.

### Confirmation of Global Latitudinal Patterns in Haplogroup Distributions at Regional Scale

At a global scale, haplogroup I (without separating off Ib, detected only in Chilean waters) was the most widespread (Figure 4A). Haplogroup II became more prevalent at higher latitudes in both hemispheres. All 10 strains originating from latitude  $>55^\circ$  were haplogroup II (5 North Sea, 1 Baltic Sea, 2 northern central Atlantic, 1 northern central Pacific, 1 northwestern Pacific), whereas haplogroup II was

**TABLE 2** | Correspondence among *cox* haplogroups and *tufA* haplogroups from SE Pacific.

<i>tufA</i> haplogr. <i>cox</i> haplogr.	I	II	III	IV	Sub-totals
I	83	0	0	1	84
Ib	47	1	0	0	48
II	1	27	0	1	29
III	0	0	0	0	0
Sub-totals	131	28	0	2	<b>Grand total: 161</b>

**TABLE 3** | Correspondence among morphotypes and *cox* haplogroups of *E. huxleyi* from SE Pacific.

Morphotype Haplogroup	A	A-CC	HC/R	B	<i>G. eric.</i>	<i>G. parv.</i>	<i>G. muel.</i>
I	30	31	5	9	1	4	0
Ib	1	1	0	48	0	0	0
II	10	3	33	22	0	0	4
Sub-total	41	35	38	79	1	4	4

mostly excluded from latitudes less than 30° N or S. Haplogroup III (*G. oceanica*) strains came from sub-tropical and tropical latitudes.

This latitudinal pattern held within the regional scale in the Southeast Pacific (Figure 4B) but appeared to be modified in relationship to patterns of upwelling. Haplogroup II dominated in the cooler nearshore waters from the strong coastal upwelling center north of Punta Lavapie (37°–36° S) to the strong upwelling center near Punta Lengua de Vaca (30° S), but was represented only 9 out of 33 strains isolated from the oceanic waters near the Juan Fernandez Archipelago (33° S, 78° W), and only 4 of 10 strains from the northern Chiloe outer coast at 42° S, south of the region where coastal upwelling is dominant.

### Global and Regional Association of Haplogroup I With Warmer, More Saline Waters and Haplogroup II With Cooler, Less Saline Waters

There was a significant negative association of haplogroup II (vs. haplogroup I) with increasing SST (Figure 4C), SSS and minimum distance from mainland coast (MDMC), while MLD was not significant (Tables 4, 5). In contrast, haplogroup Ib was not significantly associated with SST but was significantly associated negatively with SSS and MDMC and positively with MLD, but this group was only found in a small subset of locations in coastal Chile and nowhere else. Haplogroup III (vs. haplogroup I) was positively correlated with SST and SSS and negatively with MLD and MDMC, but the *p*-value for SST was just above the  $\alpha$ -threshold for significance (*p* = 0.055). Also, SST was significantly correlated with SSS and MDMC.

When only strains from the SE Pacific isolated after 2011 were considered, haplogroup II (vs. haplogroup I) was significantly negatively associated with both SST and SSS

from direct measurements of the surface water of origin (Figure 4D and Tables 6, 7).

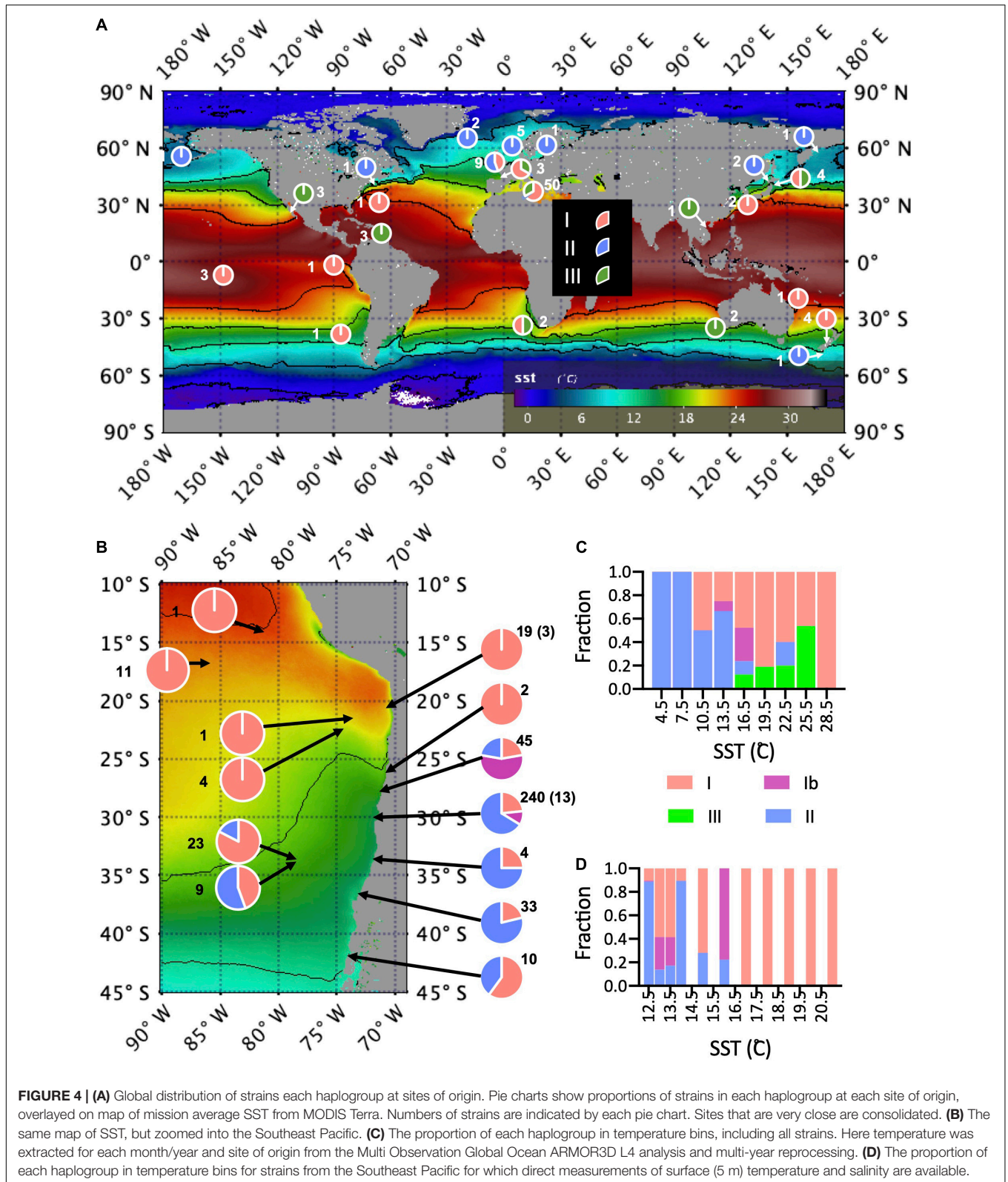
## Thermal Performance Curves and Thermal Reaction Norms

### Experiment 1: Thermal Reaction Norms Differ Among Species

In this first experiment, focused on the interspecies comparison, all analyses suggested that *G. muelleriae* had the lower thermal optima while *G. oceanica* and *G. parvula* tended to have higher thermal optima, with *E. huxleyi* intermediate (Figures 5, 6). In thermal performance curves analysis from Experiment 1, *E. huxleyi* haplogroups I and II were not significantly different (Figure 6), and so tests were repeated consolidating *E. huxleyi* haplogroups to provide more confidence in analysis of interspecific differences. None of the *G. muelleriae* strains could grow at 24°C (Figure 5E), nor could the one strain of *E. huxleyi* Ib (SEPA118), whereas all of *E. huxleyi* haplogroups I and II, *G. oceanica*, *G. parvula-ericsonii* group grew at that temperature. Three of the five *G. parvula-ericsonii*, 9 of the 11 *E. huxleyi* tested, and all *G. oceanica* could also grow at 27°C, suggesting that *G. oceanica* is typically the most warm-tolerant (Figure 6A). All *G. muelleriae* and all *E. huxleyi* grew at 8°C, while none of *G. parvula-ericsonii* or *G. oceanica* grew at that lower temperature (Figures 5, 6B). Three *G. oceanica* strains (RCC1562, RCC1803, and RCC3729) did not even grow at 12°C (Figure 5F). There was no difference detected among haplogroups or among species in the Norberg performance (height) parameter *a* (Figure 6C) except when *E. huxleyi* were consolidated, and *G. oceanica* had a significantly lower *a* than *E. huxleyi*. The TPC fits also indicated a lower thermal optima of *G. muelleriae*, and higher optima of *G. oceanica*, compared to *E. huxleyi* and other *Gephyrocapsa*, whether measured as Norberg *Z* (competitive optimum temperature) (Figure 6D) or *T<sub>opt</sub>* (temp. of max. growth rate) from TMV analysis (Supplementary Figures 14, 15). Within the *G. parvula-ericsonii* genetic group, the single *G. ericsonii* strain (SEPA516) had lower *Z* and *T<sub>opt</sub>* fits than the four *G. parvula*. The mean separation between the thermal optima of *G. muelleriae* and *G. oceanica* was 4.5°C for both *Z* and *T<sub>opt</sub>*.

The largest Norberg niche width parameter *W* was of an *E. huxleyi* SEPA81 (haplogroup II) while the narrowest was from *E. huxleyi* strain SEPA118 (the single member of haplogroup Ib in this experiment, not included in statistical tests except when *E. huxleyi* was consolidated) (Figure 6E). While both *E. huxleyi* I and II tended to have larger *W*'s than the other species, only the pairwise differences of *E. huxleyi* I with *G. oceanica* and *G. muelleriae* were significant. When *E. huxleyi* was consolidated, the difference was only significant with *G. muelleriae*.

There was no relationship between performance (*a*) and width *W* (Figure 6F). The TMV decomposition of the modes of variation, performed on all except *G. muelleriae* indicated that only 6.9% of total variation was related to a generalist-vs-specialist mode, which, while we interpret with caution as explained in the Methods, was consistent with the results from reaction norms obtained with the Norberg curve fitting.



There was a significant relationship between Norberg Z and the reconstructed SST of the month of origin (Figure 6G). However, the relationship was also significantly less than 1, with

most of the *G. oceanica* exhibiting Z's below their SST of origin, whereas all of the Southeast Pacific strains, with the exception of a single *G. muelleriae* strain, exhibited Z's above the SST of origin.

**TABLE 4 |** Mean reconstructed environmental characteristics for all strains for which *cox* haplogroup is available (from 1993).

	SST	SSS	MLD	MDMC	N
I	16.8 ± 4.9 [11.9–28.9]	35.2 ± 1.6 [33.3–39.3]	31.0 ± 29.8 [11.0–184]	267 ± 642 [0–4830]	195
Ib	15.1 ± 1.7 [12.8–16.7]	34.4 ± 0.14 [34.2–34.6]	37.3–7.6 [25.6–43.9]	25.6 ± 9.1 10.9–33.4	50
II	13.5 ± 1.6 [4.6–22.9]	34.3 ± 1.9 [6.6–36.9]	27.1 ± 7.0 [10.4–43.9]	40.0 ± 122 [0–605]	226
III	19.6 ± 4.8 [12.2–26.4]	36.4 ± 1.3 [33.4–37.6]	19.2 ± 13.6 [12.3–62.3]	82.3 ± 93.9 [0–242]	26

Given are mean ± SD and range for sea surface temperature (SST), sea surface salinity (SSS), mixed layer depth (MLD), min. distance from mainland coast (MDMC) and number of sequences (N).

### Experiment 2: Thermal Reaction Norms Differences Among *E. huxleyi* Haplogroups Isolated Together in the LowPHox I Cruise

All but two of the strains of *E. huxleyi* haplogroup I could grow at 27°C but most haplogroup Ib and II strains could not grow at that temperature (Figures 7, 8A). The differences between I vs. Ib and I vs. II were significant. All strains of the three haplogroups could grow at 8°C (Figures 7, 8B) and there were no significant differences in growth rates at that temperature. Both the Norberg model and TMV analysis produced adequate fits to TPC data. Visually, TMV analysis suggested that these strains might exhibit an inflection point in the rising portion of the TPC curves (Figure 7D). Norberg performance (*a*) was significantly lower in *E. huxleyi* Ib than in the other two haplogroups (Figure 8C). Both *Z* (Figure 8D) and *T<sub>opt</sub>* (Supplementary Figure 16) were significantly higher for haplogroup I compared to Ib and II. There were no differences between Ib and II. The mean difference between I and Ib was only 0.8°C, and only 0.7° between I and II.

Haplogroup I had a higher average *W* from the Norberg fits (Figure 8E), but the difference was not significant. The *w* parameter from TMV analysis also tended to be largest in haplogroup I, and the difference was significant in the comparison with haplogroup Ib (Supplementary Figure 16C).

This tendency was also interpreted when numerically estimating the full width at half max (FWHM) from the individual TMV curves (Supplementary Figure 16E). There were no significant trends in the Norberg height *a* vs. width *W*, either within haplogroups or considering all together (Figure 8F).

## DISCUSSION

This study greatly increased the total number of *E. huxleyi* strains from which mitochondrial and plastid phylogenies are available. This permitted confirming the previously documented latitudinal pattern at global and regional scales, including both the Northern and Southern hemisphere, and it permitted testing whether the thermal associations of haplogroups hold within the dynamics at a regional scale. The culture-dependent approach allowed us to address how well mitochondrial haplogroups associate with chloroplast haplogroups as well as morphotypes. Most importantly, we could directly test hypotheses about whether thermal reaction norms for growth determine oceanographic distributions either among *E. huxleyi* and its closest relatives or with *E. huxleyi*, among mitochondrial haplogroups. We discuss each of these points in detail below.

### Mitochondrial and Chloroplast Haplogroups in the *Emiliana-Gephyrocapsa* Complex

The mitochondrial phylogenies generated in this study, both of *cox1* and *cox3* sequences separately and of concatenated *cox1–3*, were largely consistent with expectations from previous published mitochondrial phylogenies of the *Emiliana-Gephyrocapsa* complex (Hagino et al., 2011; Bendif et al., 2014, 2016). However, with the inclusion of a larger number of strains we detected a new mitochondrial sub-clade not observed in previously studies. We assigned this new clade as haplogroup Ib. Its phylogenetic association with haplogroup I was supported by the ABGD analysis of concatenated *cox1–cox3* sequences in network analysis, which divided mitochondrial sequences into

**TABLE 5 |** Results of multinomial regression for *cox* haplogroup (rel. to haplogroup I) against reconstructed environmental parameters, for all strains for which *cox* haplogroup is available (from 1993).

		Intercept	SST	SSS	MLD	MDMC
Ib	Coef	20.5	0.139	−0.691	2.03 × 10 <sup>−2</sup>	−1.15 × 10 <sup>−2</sup>
	Std err	1.473	7.76 × 10 <sup>−2</sup>	5.16 × 10 <sup>−2</sup>	7.38 × 10 <sup>−3</sup>	5.57 × 10 <sup>−3</sup>
	Z	13.92	1.79	−13.4	2.75	−2.07
	p	0	7.41 × 10 <sup>−2</sup>	0	5.99 × 10 <sup>−3</sup>	3.84 × 10 <sup>−2</sup>
II	Coef	27.4	−0.344	−0.636	−2.56 × 10 <sup>−3</sup>	−2.63 × 10 <sup>−3</sup>
	Std err	1.55	7.41 × 10 <sup>−2</sup>	4.88 × 10 <sup>−2</sup>	7.47 × 10 <sup>−3</sup>	7.18 × 10 <sup>−4</sup>
	Z	17.73	−4.65	−13.0	−0.343	−3.66
	p	0	3.33 × 10 <sup>−6</sup>	0	0.732	2.53 × 10 <sup>−4</sup>
III	Coef	−7.66	0.164	0.127	−4.24 × 10 <sup>−2</sup>	−9.42 × 10 <sup>−3</sup>
	Std err	9.07 × 10 <sup>−3</sup>	8.56 × 10 <sup>−2</sup>	4.50 × 10 <sup>−2</sup>	2.51 × 10 <sup>02</sup>	4.30 × 10 <sup>−3</sup>
	Z	−845	1.91	2.83	−1.69	−2.19
	p	0	0.0556	4.70 × 10 <sup>−3</sup>	0.0910	0.0285

AIC = 911. Significant regressions are in black.

**TABLE 6 |** Mean SST and SSS for strains in each *cox* haplogroup originating exclusively from the upwelling center near 30° S.

	SST	SSS	N
I	13.0 ± 0.4 [12.3–14.1]	34.8–0.3 [34.4–35.2]	56
Ib	13.9 ± 1.2 [12.4–15.8]	34.7–0.3 [34.3–35.2]	25
II	12.7 ± 0.7 [12.3–15.8]	34.5 ± 0.1 [34.3–35.2]	158

**TABLE 7 |** Results of multinomial regression for *cox* haplogroup (rel. to haplogroup I) against direct measures of SST and SSS for strains from near the 30° S coastal upwelling.

		Intercept	SST	SSS
Ib	Coef	-17.9	1.07	$7.86 \times 10^{-2}$
	Std err	24.4	0.312	0.671
	Z	-0.733	3.44	0.117
	p	0.464	$5.76 \times 10^{-4}$	0.907
II	Coef	170	-0.551	-4.67
	Std err	10.7	0.258	0.320
	Z	15.8	-2.14	-14.6
	p	0	0.0326	0

AIC = 334. Significant regressions are in black.

either three or four clades. When *cox1-cox3* sequences were divided into only three clades, haplogroup Ib was within the clade of haplogroup I. Trees constructed by both Maximum Likelihood and Bayesian Inference also placed Ib as basal to haplogroup I, although with only moderate support, and the posterior probability for this placement in Bayesian Inference was low (0.75). Haplogroup Ib has not yet been observed in any strains isolated outside of Chilean coastal waters, and all but one of the Ib strains were isolated during or soon after the strong 2015–2016 El Niño event, when Ib was very common among strains isolated from 30° S and 27° S.

The culture-based approach here also allowed comparing mitochondrial and chloroplast phylogenies in a substantial set of strains. We were expecting to find a more complex relationship of mitochondrial (*cox*) and chloroplast (*tufA*) haplogroups based on the incongruence reported between organellar phylogenies (Bendif et al., 2016). Distinct mitochondrial haplogroups of *E. huxleyi* are expected to be able to interbreed or at least to have done so in the recent past, based on a phylogenomic study suggesting extensive mixing among nuclear genomes (Filatov, 2019), as well as the occurrence of strains where mitochondrial and chloroplast haplogroups contrast. However, such inter-organellar phylogenetic incongruence turned out to be rare in the *E. huxleyi* strains from the SE Pacific analyzed here. Patterns of organellar inheritance are not known in these organisms, so the pattern might imply inheritance of both organelles is preferentially from one parent following syngamy, or perhaps also a degree of post-zygotic cytonuclear incompatibility (Willett, 2011) could be important.

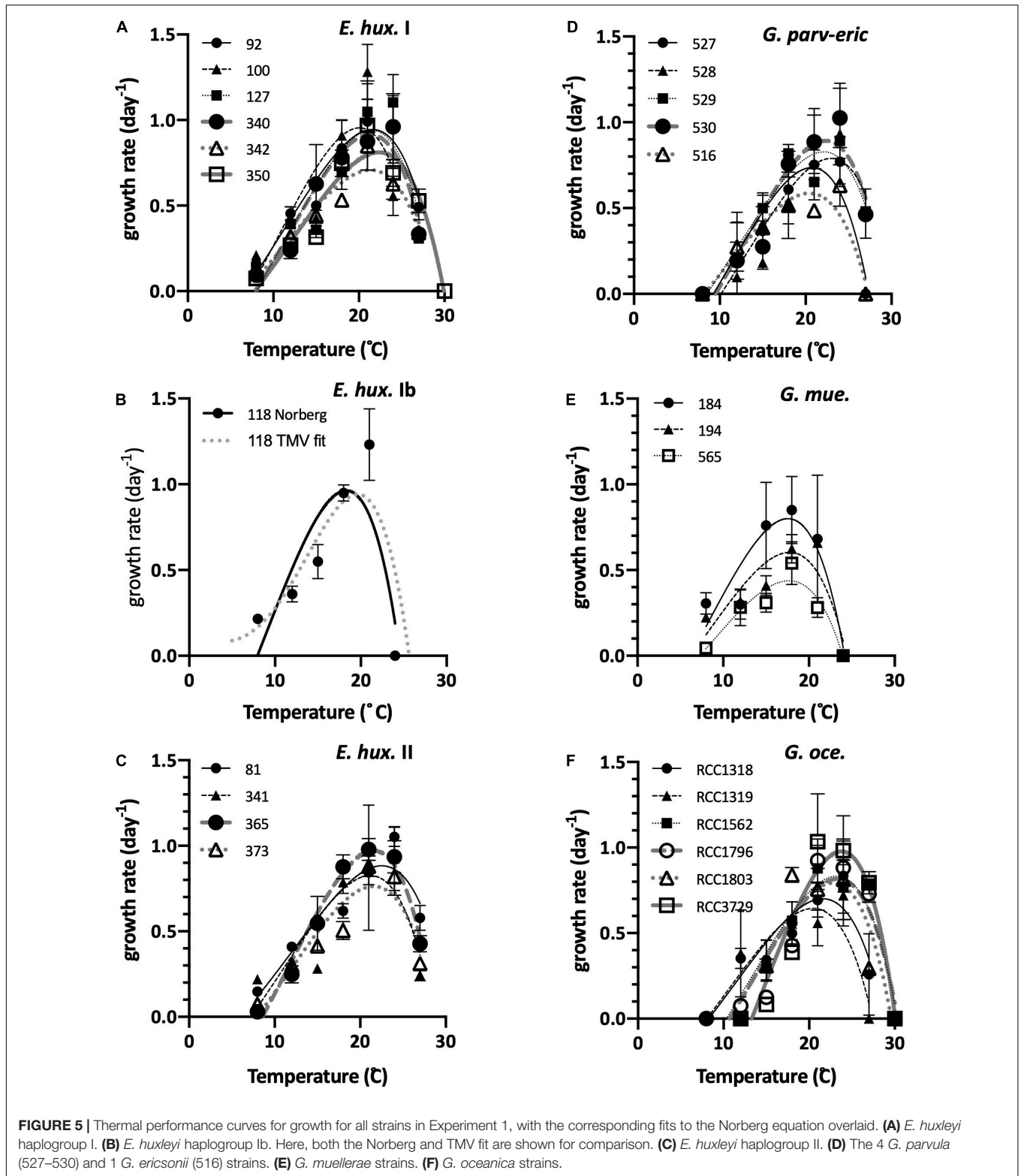
The fact that mitochondrial and chloroplast haplogroups mostly coincided permitted important simplifications in analysis

with respect to environmental data and in experimental design. For example, as no strains exhibited *cox* haplogroup I with *tufA* haplogroup II, and only 1 strain (less than 1%) exhibited *cox* haplogroup II with *tufA* haplogroup I (Table 2), it was not possible or necessary to include such combinations in the experimental determination of thermal reaction norms.

There was only a partial correspondence between morphotype and haplogroup. All haplogroups exhibited morphotypes classed in the broader B morphotype class, although we did not attempt here to distinguish among B, B/C, C, and O in this class. Distinct A morphotypes are distinguished more easily, based on whether the distal shield central area is uncovered (the original A morphotype), or covered/closed by over-calcification (here termed A-CC) or whether the distal shield elements are fused (von Dassow et al., 2018; Díaz-Rosas et al., 2021). This last is considered to be a variant of the R morphotype (Beaufort et al., 2011), but which we term HC/R to indicate that the strains from this region have a tendency for variable overgrowth of the central area (von Dassow et al., 2018; Díaz-Rosas et al., 2021), a character distinct from the original description of the R morphotype (Young et al., 2003). All of these morphotypes contained both haplogroups I and II. The original study defining mitochondrial haplotypes in *E. huxleyi* found the R morphotypes only in haplogroup I (Hagino et al., 2011), but the HC/R morphotypes from Chilean waters were preferentially group II. Morphotype is likely nuclear-determined, and is tightly associated with the nuclear GPA gene that produces a protein related to coccolith-associated polysaccharides (Schroeder et al., 2005), however, morphotype and associated genetic polymorphisms in GPA do not correspond to microsatellite population genetics (Krueger-Hadfield et al., 2014), suggesting different morphotypes may interbreed. The imperfect correspondence between morphotypes and mitochondrial haplogroups observed here thus might also support the possibility of nuclear genetic exchange among *E. huxleyi* organelle haplogroups.

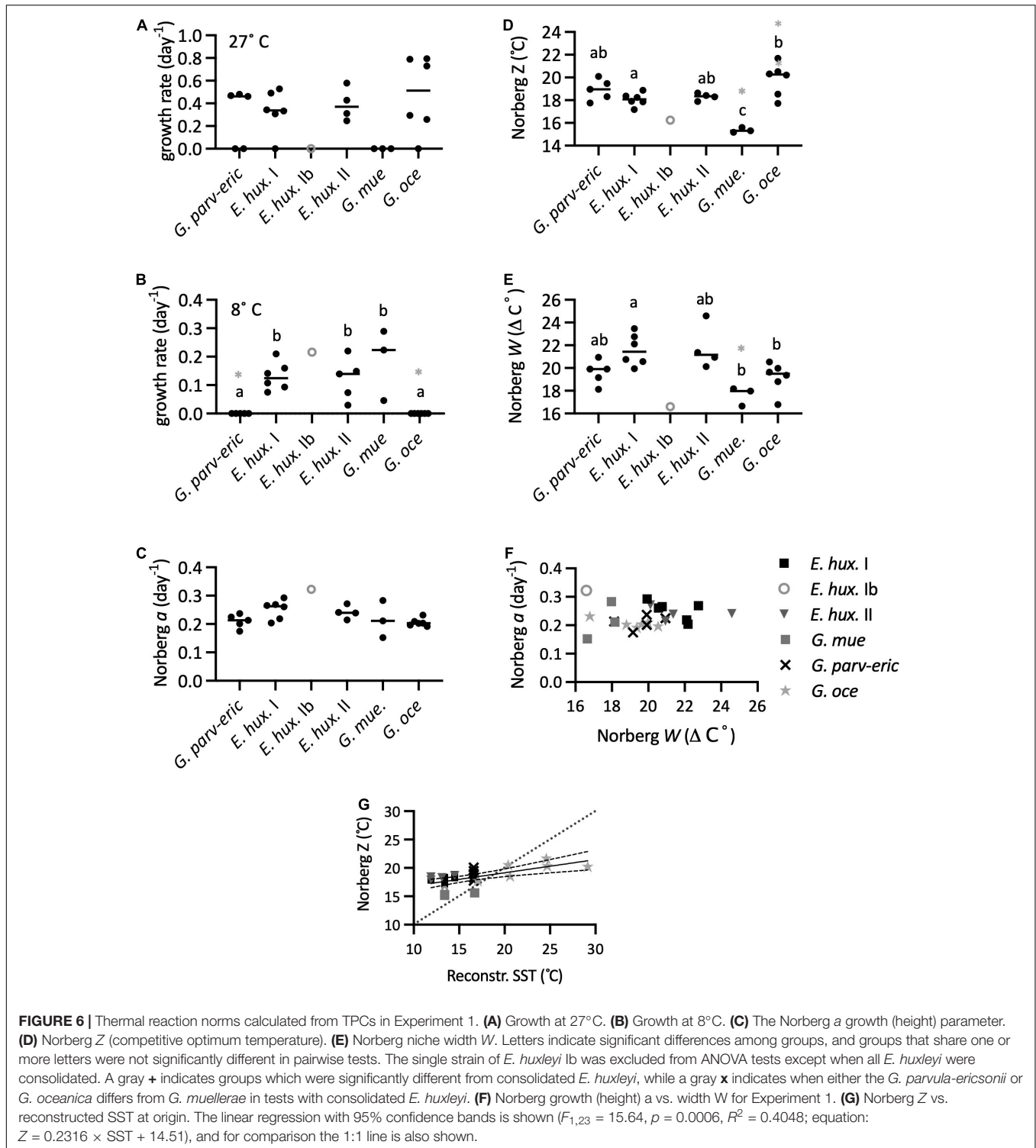
### Global Association of Haplogroup I With Low Latitudes and Warmer Waters, and Haplogroup II With Higher Latitudes and Cooler Waters

The global latitudinal pattern previously reported in *E. huxleyi* mitochondrial haplogroups was also reflected at the regional scale. The association of *E. huxleyi* II with decreasing SST, both on a global scale (using reconstructed SST) and on the regional and local scale (using direct SST measures), were consistent with temperature explaining the observed latitudinal patterns. However, the multinomial regression also detected significant associations with SSS and with distance from the coast in the global analysis. A caution is that salinity also shows a strong latitudinal gradient globally. Also, a large number of the *E. huxleyi* I *cox1* or *cox3* sequences are from the high salinity Mediterranean, but only one Mediterranean *E. huxleyi* strain was assigned as haplogroup II, and the strain origins that are farthest from continental shelves are in tropical and subtropical waters (with higher temperatures and salinities). Nevertheless, a statistically significant relationship with salinity



was also suggested at the local scale, from direct measurements of salinity among samples collected near 30° S. Indeed, strain-specific variability in reaction norms with respect to salinity has been demonstrated (Gebühr et al., 2021). Temperature

and salinity are the conservative tracers of water masses, and so other physiologically and ecologically important variables, such as nutrients or total chlorophyll, also tend to co-vary with temperature, salinity, and distance from the coast. This



emphasizes the value in experimentally determining whether physiological reaction norms in fact are consistent with patterns of specific environmental parameters at ecological scales.

The environmental associations of the new haplogroup Ib are not yet clear. So far, it has only been identified from coastal waters of central Chile. It was almost exclusively observed

during and immediately after an intense El Niño, when the northern Chilean coast typically experiences a tendency for deepening of the thermocline and warmer, more saline waters (Escribano et al., 2004; Aguilera et al., 2020). Measured SST at 30° S in Nov. 2015, when haplogroup Ib was most important, was 15.8°C, 1.7°C higher than the temperature in Nov. 2012,

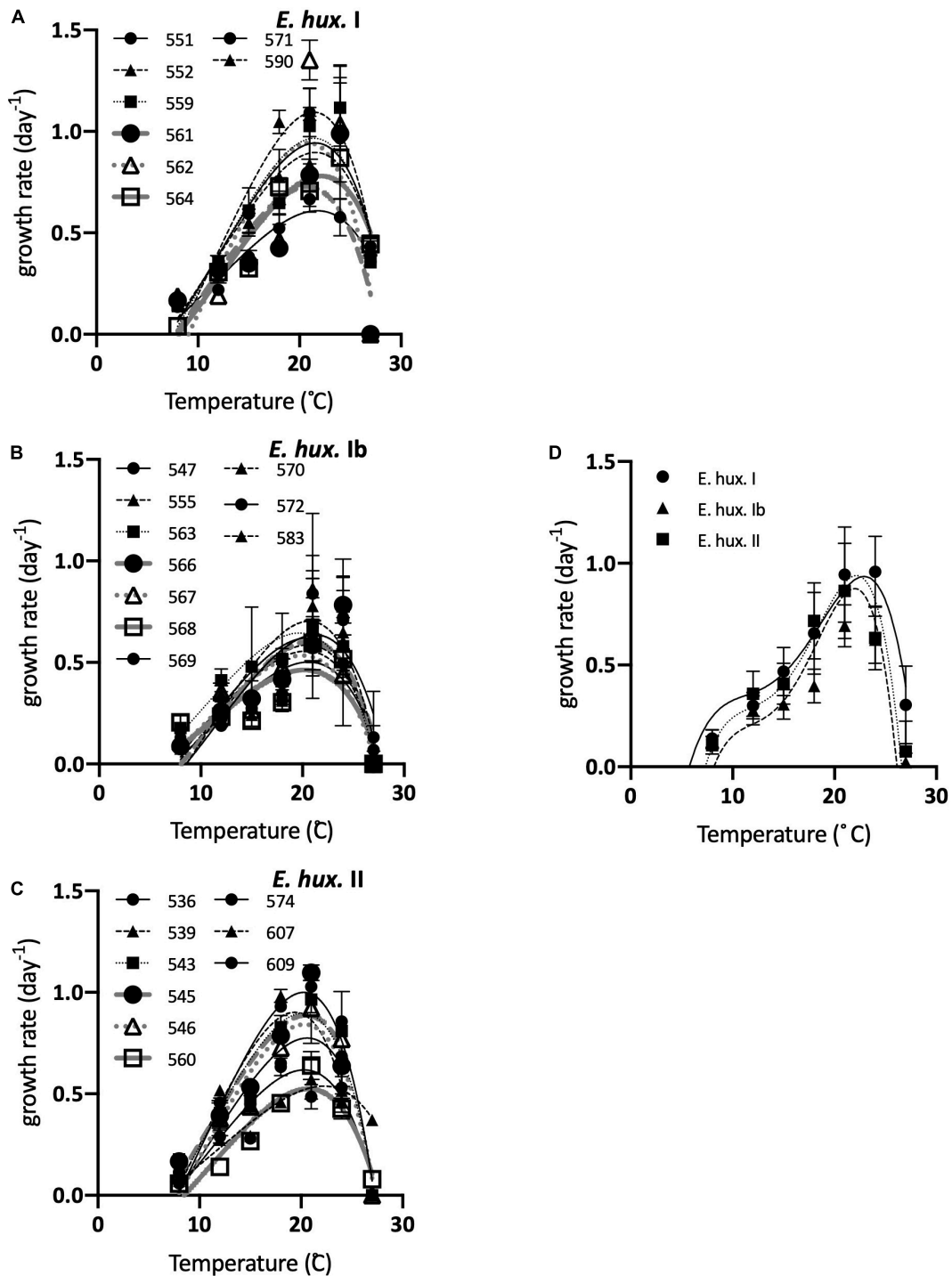
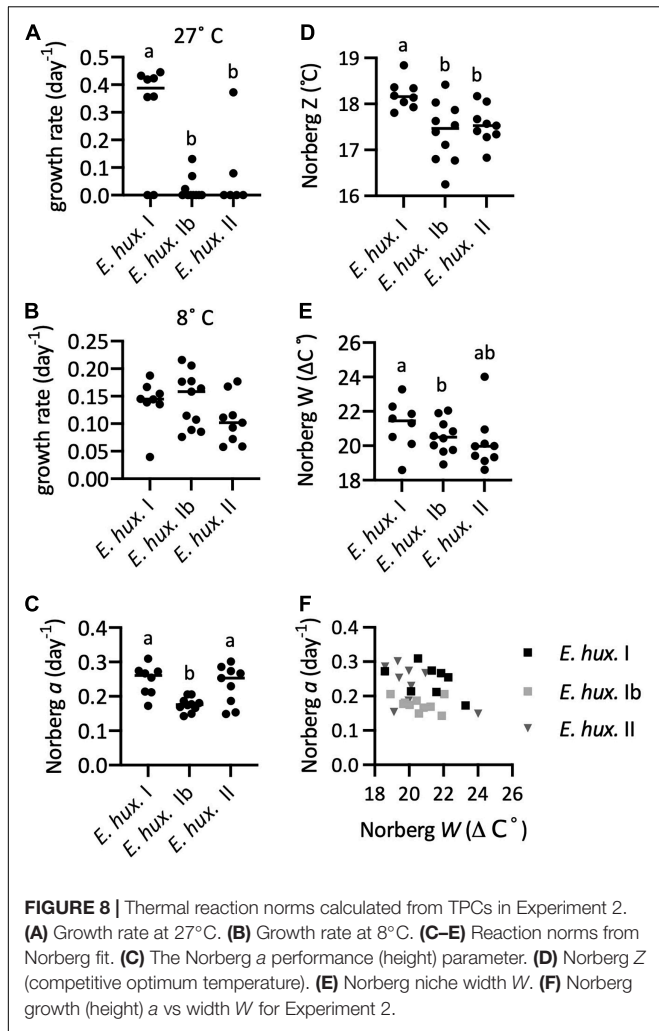


**FIGURE 7 |** Thermal performance curves for growth for all strains in Experiment 2, with the corresponding fits to the Norberg equation overlaid. **(A)** Haplogroup I. **(B)** Haplogroup Ib **(C)** Haplogroups II. **(D)** The corresponding average TMV curves overlaying the haplogroup-specific average values of growth rate at each temperature (solid line is haplogroup I, dashed line is haplogroup Ib, dotted line is haplogroup 2).

and 3.2°C higher than the average measured in Oct. 2011 (Supplementary File 2), but it was also prevalent at the end of Aug. 2016 when cooler temperatures were present, and was not found to the north in warmer waters. Continued

sampling effort, both regionally and globally and using both cultures and culture-independent methods, would be necessary to determine the geographic distribution and oceanographic preferences of this clade.



### Thermal Reaction Norms Reflect Environmental Distributions of Species

Thermal reaction norms (or at least thermal performance curves for growth, when norms were not calculated) have previously been reported for two species studied here, including a total of 17 strains of *E. huxleyi* (Conte et al., 1998; Buitenhuis et al., 2008; Zhang et al., 2014; Listmann et al., 2016; Wang et al., 2019) and two strains of *G. oceanica* (Conte et al., 1998; Buitenhuis et al., 2008). The previous studies that included *G. oceanica* showed it to be less cold-tolerant than *E. huxleyi*, but did not permit estimating  $T_{opt}$  as determined here. In the present study, *E. huxleyi* strains exhibited similar thermal reaction norms to those previously reported for this species, with the exception of one strain from the SW Indian ocean previously reported to show relative cold-intolerance and two strains from subpolar waters reported to show a much lower  $T_{opt}$ , both by Conte et al. (1998). To these species we add data from *G. muelleriae* and *G. parvula/ericsonii*, two species that were only recently isolated into culture.

Hypothesis 1, the possible role for ocean temperature in determining distributions among the different species in the

*Emiliania-Gephyrocapsa* genus, was supported by the thermal reaction norms measured in the laboratory. The species restricted to cooler waters, *G. muelleriae*, very clearly had lower temperature thermal reaction norms, both in terms of optimal temperatures and thermal limits for growth (although one of the three strains barely grew at 8°C). Consistent with their geographic distributions, the six strains of *G. oceanica* tended to show the highest optimal temperatures and thermal limits, closely followed by the five *G. parvula/ericsonii* strains. Finally, the norms for *E. huxleyi* were well above the norms for *G. muelleriae* and overlapped with the lower end of the ranges exhibited by *G. parvula/ericsonii* and *G. oceanica*. Although the differences in thermal optima (both Norberg Z, the competitive optima, and  $T_{opt}$ ) between *G. parvula/ericsonii* and *E. huxleyi* were not significant, all *E. huxleyi* tested in both experiments could grow at 8°C whereas none of the *G. parvula/ericsonii* could grow at that temperature, supporting that *G. parvula/ericsonii* is less cold-tolerant.

The competitive optimum temperature Z related linearly with the SST of origin among the *Emiliania/Gephyrocapsa* species. However, the slope was less than 1. This may reflect the larger trend among phytoplankton to exhibit higher optimum temperatures for growth than their temperature of origin except at the highest temperatures (Thomas et al., 2012). We caution that the pattern observed might be modified if there is adaptation in the lab to temperatures at which cultures are maintained prior to experiments. Nevertheless, we did not observe trends of Z or difference of Z and SST of origin vs. time in culture either within each *E. huxleyi* haplogroup or among the *G. oceanica* strains. The recent study of Anderson and Rynearson (2020) did not find a relationship between thermal optima for growth and isolation temperature among isolates of the diatom genus *Skeletonema*, despite a wider range of isolation temperatures (0 to 20°C). That difference might partly be explained by the fact that *Skeletonema* is a neritic species, and that earlier study focused on strains isolated from the Narraganset Bay. Such neritic organisms may be retained within in the bay and exposed through the year to much greater changes in temperature than coccolithophores in the *Emiliania/Gephyrocapsa* genus with a more oceanic habitat and no known benthic resting stages.

### Thermal Reaction Norms Weakly Reflect Environmental Distributions of Haplogroups Within *E. huxleyi*

To avoid local adaptation complicating the ability to detect differences among haplogroups, all but two strains tested in the Experiment 2 were from the same water sample (and the observed differences held when those two strains were excluded). Even in the same water sample, cells may have different histories, particularly in zones of intense upwelling where there is mixing of different water masses. We minimized this effect by focusing on a water sample that was well away from strong upwelling centers. The three strongest centers of upwelling along the Chilean coast are at 37° S, 30° S, and 23° S, with several weaker upwelling centers between 37° S and 30° S and at 29° S (Thiel et al., 2007), and the site at 27°S was therefore well away from these. We also

attempted to minimize the possible effects of in-culture evolution on thermal reaction norms as TPCs were fully completed within 18 months of isolation for all the *E. huxleyi* strains used in the second test.

The results presented weak support for Hypothesis 2: Among *E. huxleyi* haplogroups, the thermal reaction norms of haplogroups I and II exhibited significant differences of the expected directions only in the strains isolated in the same 2 week period and tested within 18 months of isolation. In this set, haplogroup II tended to show cold-shifted thermal reaction norms compared to haplogroup I, whether in terms of temperature of maximum growth  $T_{opt}$ , the competitive optimal temperature (Norberg's  $Z$ ), or in growth at 27°C (but not in growth at 8°C).

Despite the phylogenetic association of *E. huxleyi* haplogroup Ib with haplogroup I, its thermal reaction norms were cold-shifted to be similar to haplogroup II in the second experiment. Although the environmental distribution of Ib remains to be defined, the narrower (more specialist) thermal reaction norms of this haplogroup suggests a more specialist type, which might explain its more sporadic occurrence and apparently more restricted distribution compared to *E. huxleyi* I and II.

The differences among *E. huxleyi* I, Ib and II in Experiment 2 were relatively small, on the order of 1°C. The differences were similar to the intra-specific differences in thermal optima reported in planktonic diatoms such as *Skeletonema marinoi*, *S. pseudocostatum*, and *Thalassiosira rotula* (Boyd et al., 2013; Anderson and Rynearson, 2020), but are much smaller than those reported within *T. pseudonana* or the dinoflagellate *Akashiwo sanguinea* (Boyd et al., 2013). In the study of *E. huxleyi* strains isolated from Bergen and the Azores, a 22 degree latitudinal difference, corresponding to a 6.3°C difference in maximum monthly mean temperature or a 9.6°C difference in minimum monthly temperatures, the mean difference among populations was only 1.1°C (Zhang et al., 2014). A higher difference was reported for strains from the Indian Ocean compared to subpolar North Atlantic and North Pacific (Conte et al., 1998). Clonal selection under asexual reproduction in the lab was reported to result in a 0.7°C shift in thermal optima in *E. huxleyi* within 1200 asexual generations (Listmann et al., 2016). In that study the selection temperature used, 26°C, was near the thermal limits and well outside the range of the environment from which that original strain was isolated (Bergen). Similarly, in the diatom *T. pseudonana*, selection at 31°C (vs. 16°C) was reported to drive a nearly 2°C change in  $T_{opt}$  within 450 asexual generations (O'Donnell et al., 2018). Both of those evolution experiments imposed a very strong and constant selective pressure, both in terms of an extreme selection temperature and for maximizing growth rates (high  $r$ -selection) compared to that expected in nature, where temperatures are lower and selection for maximum growth rate (over other traits) is unlikely to be constant. Nevertheless, this emphasizes how small were the differences determined in this study among *E. huxleyi* haplogroups.

The lack of difference between *E. huxleyi* haplogroups I and II in the first experiment is unlikely to only reflect in-culture evolution, even though the strains used had been in culture

for 3–4 years by the time the preliminary experiments had started, and up to nearly 6 years when completed. Any in-culture evolution was not enough to have abolished the larger differences observed among species, where it was necessary to compare strains isolated in many different years (and including with time in other culture collections), and the single haplogroup Ib strain from 2011 that was included in the first test showed lower temperature thermal reaction norms, similar to Ib strains from 2015. Also, Conte et al. (1998) observed larger differences among five *E. huxleyi* despite many years in culture. At regional scales, temperature and salinity correlate as conservative properties of water masses (for the case of the Southeast Pacific, see, e.g., Silva et al., 2009), which also can determine or be correlated with variables such as nutrients or mixed layer depth, which may in turn influence productivity and biomass. It is possible that perhaps adaptation to these other variables, or the interaction of one or more these variables with temperature, might also influence *E. huxleyi* mitochondrial haplogroup distributions. For example, variations among *E. huxleyi* strains have been seen in reaction norms to salinity (Paasche, 2001; Gebühr et al., 2021) and in utilization of different N-sources (Strom and Bright, 2009).

Another intriguing possibility is that thermal adaptation is important, but there is nuclear gene flow between mitochondrial haplogroups I and II within *E. huxleyi*, as discussed above. Although the mitochondrial genome might contribute to thermal adaptation in other eukaryotes (Baker et al., 2019), the results suggest that the dominant control is nuclear-encoded in *Emiliana-Gephyrocapsa*. In that case, the present latitudinal distributions of the haplogroups might represent a historical association between organelle haplogroups and thermal adaptations, perhaps dating from earlier introgression events between *E. huxleyi* and other *Gephyrocapsa* species as hypothesized by Bendif et al. (2016). In regions where the haplogroups overlap, exchange of nuclear genes among *E. huxleyi* as well as local adaptation might then be erasing the association of organellar history with thermal traits.

## Does a Generalist-Specialist Trade-off With Respect to Thermal Reaction Norms Affect the Distributions of *E. huxleyi* vs. *Gephyrocapsa* Species?

Generalists are species which can occupy broad niches (diverse habitats) while specialists occupy more narrow niches, which may reflect wider or narrower physiological tolerance ranges, respectively (Futuyma and Moreno, 1988; Sriswasdi et al., 2017). Based on the wide geographical distribution of *E. huxleyi* (Paasche, 2001; Winter et al., 2014) and the much more restricted distributions of its closest relatives (*Gephyrocapsa*) in the present ocean (McIntyre et al., 1970; Bollmann and Klaas, 2008), *E. huxleyi* would be considered a generalist while the *Gephyrocapsa* may be specialists. Although it is only one of the multiple abiotic and biotic dimensions over which niches are defined (Colwell and Rangel, 2009), temperature is a dominant variable controlling biochemistry and physiology so is expected to be fundamental in the distributions of organisms, ranging

from microorganisms to ectothermic vertebrates (Eppley, 1972; Angilletta et al., 2003; Norberg, 2004; Logan and Cox, 2020). One of the principal classes of evolutionary trade-offs considered to underly species distributions is the generalist-vs.-specialist trade-off, and it has long been expected that this trade-off should be apparent as an inverse relationship between the height and width of thermal performance curves (Angilletta et al., 2003; Izem and Kingsolver, 2005; Buckley and Kingsolver, 2021). The width of the thermal niche has been speculated to play a key role in phytoplankton distributions (Boyd et al., 2013).

Some support was provided for Hypothesis 3 (wider thermal niche of *E. huxleyi* explaining its broader latitudinal distribution): Haplogroup I of *E. huxleyi* did exhibit a broader thermal (fundamental) niche in the laboratory in comparison to the *Gephyrocapsa* species and has the widest latitudinal range compared to the other *E. huxleyi* haplogroups and the other species. Nevertheless, the newly detected mitochondrial clade Ib of *E. huxleyi* exhibited a narrower thermal niche in both experiments (although only a single strain was available in the first experiment), and so far it has been identified only between 30°S and 27°S on the Chilean coast. Also, although all the *E. huxleyi* strains reported here (as well as in most other studies) grew at 8°C, Conte et al. (1998) reported that a strain from the SW Indian Ocean could not grow at 9°C, while strains from the subpolar Pacific and from Norway had an apparent  $T_{opt}$  below 20°C and lower thermal tolerance compared to other *E. huxleyi*. That shows that some *E. huxleyi* strains can exhibit thermal reaction norms outside the ranges observed here and in the other studies cited, so regional thermal adaptation also contributes to the broad distribution of *E. huxleyi*. Likewise, some *E. huxleyi*, such as haplogroup Ib, do exhibit narrower thermal niche breadths. Thus, the broad latitudinal distribution of *E. huxleyi* can partly be explained by such thermal reaction norm variation within the species (Hypothesis 4).

There was no significant tendency for strains or species with narrower thermal performance curves (or narrower tolerances) to have higher maximum growth rates, either as absolute maximum growth rates (in units of 1/time), or normalized to the Eppley Curve to adjust for the fact that the highest possible maximum growth rates are expected to be higher at higher temperatures in the range of interest here (Eppley, 1972). Previous studies comparing phytoplankton thermal reaction norms across broad phylogenetic groups have also not detected such a relationship (Thomas et al., 2012; Boyd et al., 2013; Anderson and Rynearson, 2020). In part, it may be difficult to estimate well the width parameters (or difference between critical minimum and maximum temperatures), as discussed by Boyd et al. (2013). Nevertheless, as several studies have not detected such a tradeoff, temperature and thermal reaction norms alone may not be sufficient to explain wider or narrower species distributions in phytoplankton. Physiologically, interactions among temperature and other parameters such as salinity, light, nutrients or CO<sub>2</sub> might be important (Feng et al., 2008). Analysis of distributions of *E. huxleyi* morphotypes and related *Gephyrocapsa* species in the Southeast Pacific showed that realized niches could be wide with respect to some parameters (e.g., pH and pCO<sub>2</sub>) but narrow with respect to others (e.g.,

temperature, salinity, and calcite saturation state) (Díaz-Rosas et al., 2021). Variable temperatures can negatively affect growth rate (Wang et al., 2019) and might be more important as a driver of adaptation in nature. Thus, although we did not detect a generalist-specialist trade-off in lab tests of reaction norms to a single parameter, such a trade-off in a multidimensional niche space might still be necessary to explain why there were times and locations where specialists appeared dominant, e.g., *E. huxleyi* haplogroup Ib at 27° S in 2015 (this study) or *G. parvula* at 20.7° S in 2013 (Bendif et al., 2016).

## Consequences of a Warming Ocean for the *Emiliana/Gephyrocapsa* Genus

As the global ocean warms, the habitat thermally permissive for *G. oceanica* and *G. parvula/ericsonii* is expected to expand poleward. In the case of *G. oceanica*, its thermal optima are near or even below the SST at the warmer end of its range, so the low latitude end of its range should also move poleward. *Gephyrocapsa parvula/ericsonii* may partially follow the border of the South Pacific Gyre (McIntyre et al., 1970; Bollmann and Klaas, 2008), and this gyre is becoming larger (Polovina et al., 2008). In the case of *G. muelleriae*, Eastern boundaries of ocean basins may experience intensification of upwelling-favorable coastal winds, resulting in lower temperatures (Sydeman et al., 2014), a phenomenon documented to be occurring in the Southeast Pacific (e.g., Schneider et al., 2017). This latter process might permit *G. muelleriae* to maintain or even extend its range equatorward, confined to the narrow coastal zone with cooler upwelling water, while this trend continues. Nevertheless, in these waters, *G. muelleriae* appears to exist in lower abundance compared to *E. huxleyi* (Díaz-Rosas et al., 2021). Overall, *E. huxleyi* behaves as a generalist and is capable of rapid adaptation, and the lack of evidence for strong differentiation in thermal niches between haplogroups suggest that gene flow may be high among *E. huxleyi* when populations with different adaptations mix. Thus, *E. huxleyi* might be expected to increase its dominance over its close relatives in the changing ocean.

## SUMMARY

Thermal reaction norms in culture did reflect the environmental distributions among closely related species of the *Emiliana/Gephyrocapsa* complex. Average thermal optima and tolerances, in order from coolest tolerant to warmest tolerant, were: *G. muelleriae*, *E. huxleyi*, *G. parvula/ericsonii*, and *G. oceanica*, matching the reported environmental distributions of these species. However, within *E. huxleyi*, although the direction of the difference in thermal optima between haplogroups I and II matched the prediction, the effect was very small. Present differences in thermal reaction norms might not be sufficient to explain the differences in latitudinal distributions of organellar haplogroups within *E. huxleyi*. The cosmopolitan distribution of *E. huxleyi* appears to reflect that it contains both generalist (e.g., *cox* haplogroup I) and specialist (e.g., *cox* haplogroup Ib) types. No trade-off was detected

between thermal niche width and maximum performance at optimal temperatures, but types with narrower thermal niches (thermal specialists) were occasionally more abundant compared to thermal generalists in some samples.

## DATA AVAILABILITY STATEMENT

The sequences generated in this study have been deposited in GenBank and the accession numbers are available in the **Supplementary Material**. The strains are in public algal culture collections (Roscoff Culture Collection in France and South East Pacific Algae in Chile) as indicated in **Supplementary Files 1, 3**.

## AUTHOR CONTRIBUTIONS

PD designed and led the study, performed curve fitting and statistical analysis, performed morphological classification from scanning electron microscopy images, and wrote the manuscript. SP performed sequencing of *cox1*, *cox3*, and *tufA* markers as well as initial genetic analysis, as well as electron microscopy and morphological classification of strains collected in 2016. SA-S performed final phylogenetic analysis (ML and Bayesian trees, ABGD). EV-S performed initial TPC trials and testing of growth in flasks vs. tubes. PM performed TPC curves and initial curve fitting and statistical analysis. All authors contributed to the article and approved the submitted version.

## FUNDING

Funding was provided by the Agencia Nacional de Investigación y Desarrollo (Ministerio de Ciencia, Tecnología, Conocimiento, e Innovación, Chile) through grants FONDECYT 1141106, FONDECYT 1181614, and the Millennium Institute of Oceanography (ICN12\_019-IMO). Additional funding (travel of SP and electron microscopy and sequencing of *E. huxleyi* strains collected in 2016) was provided by the Centre National de la

Recherche Scientifique (France) through IRL 3614. FONDEQUIP EQM130267 provided funds for the purchase of the InFlux Cell Sorter. Some of the SEM work was performed in the CIEN-UC facility funded by Proyecto Fondecuip EQM150101.

## ACKNOWLEDGMENTS

We thank V. Flores for processing many of the SEM samples and personnel of the SEPA collection for provision of or acquisition of biological resources (strains) used in this work. We also thank M. Valero for helpful comments on a draft of the manuscript. We graciously acknowledge the support of I. Probert and the RCC for providing strains, as well as the RCC website for information on origins of strains in the RCC.

## SUPPLEMENTARY MATERIAL

The Supplementary Material for this article can be found online at: <https://www.frontiersin.org/articles/10.3389/fmars.2021.785763/full#supplementary-material>

**Supplementary File 1** | Excel file relating the primary strain ID, alias (e.g., synonymous strain id), origin (site identifier used in **Supplementary File 2**, latitude, longitude), date, gene identifications, and *cox* and *tufA* haplotypes and haplogroups.

**Supplementary File 2** | Excel file indicating sites or origin for which strains (or strain sequences) used in this study, as well as minimum distance from mainland coast, reconstructed SST, SSS, MLD (from MULTIOBS\_GLO\_PHY\_TSUV\_3D\_MYNRT\_015\_012 product) and, when available, direct measurements of SST and SSS. (Excel format).

**Supplementary File 3** | Excel file indicating strains from the Chilean collection deposited in the Roscoff Culture Collection, with corresponding RCC designation. Possible duplicates are indicated.

**Supplementary File 4** | Excel file giving for each experiment, the average growth rates followed in the next column by standard deviations for each strain at each temperature. For many cases where the final growth rate is 0, there is no standard deviation registered because there was insufficient biomass from the acclimation cultures (as they did not grow) to inoculate replicate experimental cultures.

## REFERENCES

- Aguilera, V. M., Vargas, C. A., and Dewitte, B. (2020). Intraseasonal hydrographic variations and nearshore carbonates system off Northern Chile during the 2015 El Niño event. *J. Geophys. Res. Biogeosci.* 125:e2020JG005704. doi: 10.1029/2020JG005704
- Anderson, S. I., and Rynearson, T. A. (2020). Variability approaching the thermal limits can drive diatom community dynamics. *Limnol. Oceanogr.* 65, 1961–1973. doi: 10.1002/lno.11430
- Angilletta, M. J., Wilson, R. S., Navas, C. A., and James, R. S. (2003). Tradeoffs and the evolution of thermal reaction norms. *Trends Ecol. Evol.* 18, 234–240. doi: 10.1016/S0169-5347(03)00087-9
- Baker, E. P., Peris, D., Moriarty, R. V., Li, X. C., Fay, J. C., and Hittinger, C. T. (2019). Mitochondrial DNA and temperature tolerance in lager yeasts. *Sci. Adv.* 5:eav1869. doi: 10.1126/sciadv.aav1869
- Bandelt, H. J., Forster, P., and Rohlf, A. (1999). Median-joining networks for inferring intraspecific phylogenies. *Mol. Biol. Evol.* 16, 37–48. doi: 10.1093/oxfordjournals.molbev.a026036
- Beaufort, L., Probert, I., de Garidel-Thoron, T., Bendif, E. M., Ruiz-Pino, D., Metzl, N., et al. (2011). Sensitivity of coccolithophores to carbonate chemistry and ocean acidification. *Nature* 476, 80–83.
- Bendif, E. M., Nevado, B., Wong, E. L. Y., Hagino, K., Probert, I., Young, J. R., et al. (2019). Repeated species radiations in the recent evolution of the key marine phytoplankton lineage Gephyrocapsa. *Nat. Commun.* 10:4234. doi: 10.1038/s41467-019-12169-7
- Bendif, E. M., Probert, I., Carmichael, M., Romac, S., Hagino, K., and de Vargas, C. (2014). Genetic delineation between and within the widespread coccolithophore morpho-species *Emiliana huxleyi* and *Gephyrocapsa oceanica* (Haptophyta). *J. Phycol.* 50, 140–148. doi: 10.1111/jpy.12147
- Bendif, E. M., Probert, I., Díaz-Rosas, F., Thomas, D., van den Engh, G., Young, J. R., et al. (2016). Recent reticulate evolution in the ecologically dominant lineage of coccolithophores. *Front. Microbiol.* 7:784. doi: 10.3389/fmicb.2016.00784
- Bendif, E. M., Probert, I., Young, J. R., and von Dassow, P. (2015). Morphological and Phylogenetic characterization of new Gephyrocapsa Isolates suggests introgressive hybridization in the Emiliana/Gephyrocapsa complex (Haptophyta). *Protist* 166, 323–336. doi: 10.1016/j.protis.2015.05.003

- Bollmann, J. (1997). Morphology and biogeography of *Gephyrocapsa* coccoliths in Holocene sediments. *Mar. Micropaleontol.* 29, 319–350. doi: 10.1016/S0377-8398(96)00028-X
- Bollmann, J., and Klaas, C. (2008). Morphological variation of *Gephyrocapsa oceanica* Kamptner 1943 in plankton samples: implications for ecologic and taxonomic interpretations. *Protist* 159, 369–381. doi: 10.1016/j.protis.2008.02.001
- Boyd, P. W., Rynearson, T. A., Armstrong, E. A., Fu, F., Hayashi, K., Hu, Z., et al. (2013). Marine phytoplankton temperature versus growth responses from polar to tropical waters – Outcome of a scientific community-wide study. *PLoS One* 8:e63091. doi: 10.1371/journal.pone.0063091
- Brand, L. E. (1982). Genetic variability and spatial patterns of genetic differentiation in the reproductive rates of the marine coccolithophores *Emiliana huxleyi* and *Gephyrocapsa oceanica*. *Limnol. Oceanogr.* 27, 236–245.
- Brand, L. E., Guillard, R. R. L., and Murphy, L. S. (1981). A method for the rapid and precise determination of acclimated phytoplankton reproduction rates. *J. Plankton Res.* 3, 193–201.
- Buckley, L. B., and Kingsolver, J. G. (2021). Evolution of thermal sensitivity in changing and variable climates. *Annu. Rev. Ecol. Syst.* 52, 563–586. doi: 10.1146/annurev-ecolsys-011521-102856
- Buitenhuis, E. T., Pangerc, T., Franklin, D. J., Le Quéré, C., and Malin, G. (2008). Growth rates of six coccolithophorid strains as a function of temperature. *Limnol. Oceanogr.* 53, 1181–1185. doi: 10.4319/lo.2008.53.3.1181
- Camus, M. F., Wolff, J. N., Sgrò, C. M., and Dowling, D. K. (2017). Experimental support that natural selection has shaped the latitudinal distribution of mitochondrial haplotypes in Australian *Drosophila melanogaster*. *Mol. Biol. Evol.* 34, 2600–2612. doi: 10.1093/molbev/msx184
- Colwell, R. K., and Rangel, T. F. (2009). Hutchinson's duality: the once and future niche. *Proc. Natl. Acad. Sci. U.S.A.* 106, 19651–19658. doi: 10.1073/pnas.0901650106
- Conte, M. H., Thompson, A., Lesley, D., and Harris, R. P. (1998). Genetic and physiological influences on the alkenone/alkenoate versus growth temperature relationship in *Emiliana huxleyi* and *Gephyrocapsa oceanica*. *Geochim. Cosmochim. Acta* 62, 51–68. doi: 10.1016/S0016-7037(97)00327-X
- Díaz-Rosas, F., Alves-de-Souza, C., Alarcón, E., Menschel, E., González, H. E., Torres, R., et al. (2021). Abundances and morphotypes of the coccolithophore *Emiliana huxleyi*; in southern Patagonia compared to neighboring oceans and northern-hemisphere fjords. *Biogeosciences* 18, 5465–5489. doi: 10.5194/bg-2020-449
- Echeveste, P., Croot, P., and von Dassow, P. (2018). Differences in the sensitivity to Cu and ligand production of coastal vs offshore strains of *Emiliana huxleyi*. *Sci. Total Environ.* 625, 1673–1680. doi: 10.1016/j.scitotenv.2017.10.050
- Eppley, R. W. (1972). Temperature and phytoplankton growth in the sea. *Fish. Bull.* 20, 1063–1085.
- Escribano, R., Daneri, G., Fariás, L., Gallardo, V. A., González, H. E., Gutiérrez, D., et al. (2004). Biological and chemical consequences of the 1997–1998 El Niño in the Chilean coastal upwelling system: a synthesis. *Deep Sea Res. II Top. Stud. Oceanogr.* 51, 2389–2411. doi: 10.1016/j.dsr.2.2004.08.011
- Feng, Y., Roleda, M. Y., Armstrong, E., Boyd, P. W., and Hurd, C. L. (2017). Environmental controls on the growth, photosynthetic and calcification rates of a Southern Hemisphere strain of the coccolithophore *Emiliana huxleyi*: environmental controls on *E. huxleyi* physiology. *Limnol. Oceanogr.* 62, 519–540. doi: 10.1002/lno.10442
- Feng, Y., Warner, M. E., Zhang, Y., Sun, J., Fu, F. X., Rose, J. M., et al. (2008). Interactive effects of increased pCO<sub>2</sub>, temperature and irradiance on the marine coccolithophore *Emiliana huxleyi* (Prymnesiophyceae). *Eur. J. Phycol.* 43, 87–98.
- Field, C. B., Behrenfeld, M. J., Randerson, J. T., and Falkowski, P. (1998). Primary production of the biosphere: integrating terrestrial and oceanic components. *Science* 281, 237–240. doi: 10.1126/science.281.5374.237
- Filatov, D. A. (2019). Extreme Lewontin's Paradox in ubiquitous marine phytoplankton Species. *Mol. Biol. Evol.* 36, 4–14. doi: 10.1093/molbev/msy195
- Futuyama, D. J., and Moreno, G. (1988). The evolution of ecological specialization. *Annu. Rev. Ecol. Syst.* 19, 207–233. doi: 10.1146/annurev.es.19.110188.001231
- Gattuso, J.-P., Magnan, A., Billé, R., Cheung, W. W. L., Howes, E. L., Joos, F., et al. (2015). Contrasting futures for ocean and society from different anthropogenic CO<sub>2</sub> emissions scenarios. *Science* 349:aac4722. doi: 10.1126/science.aac4722
- Gebühr, C., Sheward, R. M., Herrle, J. O., and Bollmann, J. (2021). Strain-specific morphological response of the dominant calcifying phytoplankton species *Emiliana huxleyi* to salinity change. *PLoS One* 16:e0246745. doi: 10.1371/journal.pone.0246745
- Guinehut, S., Dhomp, A.-L., Larnicol, G., and Le Traon, P.-Y. (2012). High resolution 3-D temperature and salinity fields derived from in situ and satellite observations. *Ocean Sci.* 8, 845–857. doi: 10.5194/os-8-845-2012
- Hagino, K., Bendif, E. M., Young, J. R., Kogame, K., Probert, I., Takano, Y., et al. (2011). New evidence for morphological and genetic variation in the cosmopolitan coccolithophore *Emiliana huxleyi* (Prymnesiophyceae) from the COX1B ATP4 genes. *J. Phycol.* 47, 164–176.
- Healey, A., Furtado, A., Cooper, T., and Henry, R. J. (2014). Protocol: a simple method for extracting next-generation sequencing quality genomic DNA from recalcitrant plant species. *Plant Methods* 10:21. doi: 10.1186/1746-4811-10-21
- Hoegh-Guldberg, O., and BRJuno, J. F. (2010). The impact of climate change on the world's marine ecosystems. *Science* 328, 1523–1528. doi: 10.1126/science.1189930
- Izem, R., and Kingsolver, J. G. (2005). Variation in continuous reaction norms: quantifying directions of biological interest. *Am. Nat.* 166, 277–289. doi: 10.1086/431314
- Krueger-Hadfield, S. A., Balestreri, C., Schroeder, J., Highfield, A., Helaouët, P., Allum, J., et al. (2014). Genotyping an *Emiliana huxleyi*; (Prymnesiophyceae) bloom event in the North Sea reveals evidence of asexual reproduction. *Biogeosciences* 11, 5215–5234. doi: 10.5194/bg-11-5215-2014
- Laws, E. A., Falkowski, P. G., Smith, W. O., Ducklow, H., and McCarthy, J. J. (2000). Temperature effects on export production in the open ocean. *Glob. Biogeochem. Cycles* 14, 1231–1246. doi: 10.1029/1999GB001229
- Leigh, J. W., and Bryant, D. (2015). POPART?: full-feature software for haplotype network construction. *Methods Ecol. Evol.* 6, 1110–1116. doi: 10.1111/2041-210X.12410
- Listmann, L., LeRoch, M., Schlüter, L., Thomas, M. K., and Reusch, T. B. H. (2016). Swift thermal reaction norm evolution in a key marine phytoplankton species. *Evol. Appl.* 9, 1156–1164. doi: 10.1111/eva.12362
- Logan, M. L., and Cox, C. L. (2020). genetic constraints, transcriptome plasticity, and the evolutionary response to climate change. *Front. Genet.* 11:538226. doi: 10.3389/fgene.2020.538226
- McIntyre, A., Bé, A. W. H., and Roche, M. B. (1970). Modern Pacific Coccolithophorida: a paleontological thermometer. *Trans. N. Y. Acad. Sci.* 32, 720–731. doi: 10.1111/j.2164-0947.1970.tb02746.x
- Medlin, L. K., Barker, G. L. A., Campbell, L., Green, J. C., Hayes, P. K., Marie, D., et al. (1996). Genetic characterisation of *Emiliana huxleyi* (Haptophyta). *J. Mar. Syst.* 9, 13–31.
- Meyer, J., and Riebesell, U. (2015). Reviews and syntheses: responses of coccolithophores to ocean acidification: a meta-analysis. *Biogeosciences* 12, 1671–1682. doi: 10.5194/bg-12-1671-2015
- Mishmar, D., Ruiz-Pesini, E., Golik, P., Macaulay, V., Clark, A. G., Hosseini, S., et al. (2003). Natural selection shaped regional mtDNA variation in humans. *Proc. Natl. Acad. Sci.* 100, 171–176. doi: 10.1073/pnas.0136972100
- Mulet, S., Rio, M.-H., Mignot, A., Guinehut, S., and Morrow, R. (2012). A new estimate of the global 3D geostrophic ocean circulation based on satellite data and in-situ measurements. *Deep Sea Res. Part II Top. Stud. Oceanogr.* 7, 70–81. doi: 10.1016/j.dsr.2.2012.04.012
- Norberg, J. (2004). Biodiversity and ecosystem functioning: a complex adaptive systems approach. *Limnol. Oceanogr.* 49, 1269–1277. doi: 10.4319/lo.2004.49.4\_part\_2.1269
- O'Donnell, D. R., Hamman, C. R., Johnson, E. C., Kremer, C. T., Klausmeier, C. A., and Litchman, E. (2018). Rapid thermal adaptation in a marine diatom reveals constraints and trade-offs. *Glob. Change Biol.* 24, 4554–4565. doi: 10.1111/gcb.14360
- Okada, H., and McIntyre, A. (1977). Modern coccolithophores of the Pacific and North Atlantic Oceans. *Micropaleontology* 23, 1–55. doi: 10.2307/1485309
- Paasche, E. (2001). A review of the coccolithophorid *Emiliana huxleyi* (Prymnesiophyceae), with particular reference to growth, coccolith formation, and calcification-photosynthesis interactions. *Phycologia* 40, 503–529.
- Polovina, J. J., Howell, E. A., and Abecassis, M. (2008). Ocean's least productive waters are expanding. *Geophys. Res. Lett.* 35:L03618. doi: 10.1029/2007GL031745

- Pörtner, H.-O., Roberts, D. C., Masson-Delmotte, V., Zhai, P., Tignor, M., Poloczanska, E., et al. (2019). *IPCC, 2019: IPCC Special Report on the Ocean and Cryosphere in a Changing Climate*. Geneva: Intergovernmental Panel on Climate Change.
- Puillandre, N., Lambert, A., Brouillet, S., and Achaz, G. (2012). ABGD, automatic barcode gap discovery for primary species delimitation: ABGD, AUTOMATIC BARCODE GAP DISCOVERY. *Mol. Ecol.* 21, 1864–1877. doi: 10.1111/j.1365-294X.2011.05239.x
- R Core Team (2020). *R: A Language and Environment for Statistical Computing*. Geneva: R Core Team.
- Raffi, I., Backman, J., Fornaciari, E., Pälike, H., Rio, D., Lourens, L., et al. (2006). A review of calcareous nannofossil astrobiochronology encompassing the past 25 million years. *Quat. Sci. Rev.* 25, 3113–3137.
- Read, B. A., Kegel, J., Klute, M. J., Kuo, A., Lefebvre, S. C., Maumus, F., et al. (2013). Pan genome of the phytoplankton *Emiliana* underpins its global distribution. *Nature* 499, 209–213. doi: 10.1038/nature12221
- Ripplery, B., and Venebles, W. (2021). *Feed-Forward Neural Networks and Multinomial Log-Linear Models*.
- Schneider, W., Donoso, D., Garcés-Vargas, J., and Escribano, R. (2017). Water-column cooling and sea surface salinity increase in the upwelling region off central-south Chile driven by a poleward displacement of the South Pacific High. *Prog. Oceanogr.* 151, 38–48. doi: 10.1016/j.pocean.2016.11.004
- Schroeder, D. C., Biggi, G. F., Hall, M., Davy, J., Martinez, J. M., Richardson, A. J., et al. (2005). A genetic marker to separate *Emiliana huxleyi* (Prymnesiophyceae) morphotypes. *J. Phycol.* 41, 874–879. doi: 10.1111/j.1529-8817.2005.04188.x
- Silva, N., Rojas, N., and Fedele, A. (2009). Water masses in the Humboldt Current System: properties, distribution, and the nitrate deficit as a chemical water mass tracer for Equatorial Subsurface Water off Chile. *Deep Sea Res. Part II Top. Stud. Oceanogr.* 56, 1004–1020. doi: 10.1016/j.dsr2.2008.12.013
- Sriswasdi, S., Yang, C., and Iwasaki, W. (2017). Generalist species drive microbial dispersion and evolution. *Nat. Commun.* 8:1162. doi: 10.1038/s41467-017-01265-1
- Strom, S. L., and Bright, K. J. (2009). Inter-strain differences in nitrogen use by the coccolithophore *Emiliana huxleyi*, and consequences for predation by a planktonic ciliate. *Harmful Algae* 8, 811–816.
- Sydeman, W. J., García-Reyes, M., Schoeman, D. S., Rykaczewski, R. R., Thompson, S. A., Black, B. A., et al. (2014). Climate change and wind intensification in coastal upwelling ecosystems. *Science* 345, 77–80. doi: 10.1126/science.1251635
- Thiel, M., Macaya, E., Acuña, E., Arntz, W., Bastias, H., Brokordt, K., et al. (2007). The Humboldt Current System of northern and central Chile: oceanographic processes, ecological interactions and socioeconomic feedback. *Oceanogr. Mar. Biol.* 45, 195–345. doi: 10.1201/9781420050943.ch6
- Thomas, M. K., Kremer, C. T., Klausmeier, C. A., and Litchman, E. (2012). A Global Pattern of thermal adaptation in marine phytoplankton. *Science* 338, 1085–1088. doi: 10.1126/science.1224836
- Toseland, A., Daines, S. J., Clark, J. R., Kirkham, A., Strauss, J., Uhlig, C., et al. (2013). The impact of temperature on marine phytoplankton resource allocation and metabolism. *Nat. Clim. Change* 3, 979–984. doi: 10.1038/nclimate1989
- von Dassow, P., Díaz-Rosas, F., Bendif, E. M., Gaitán-Espitia, J.-D., Mella-Flores, D., Rokitta, S., et al. (2018). Over-calcified forms of the coccolithophore *Emiliana huxleyi* in high-CO<sub>2</sub> waters are not preadapted to ocean acidification. *Biogeosciences* 15, 1515–1534. doi: 10.5194/bg-15-1515-2018
- von Dassow, P., John, U., Ogata, H., Probert, I., Bendif, E. M., Kegel, J. U., et al. (2015). Life-cycle modification in open oceans accounts for genome variability in a cosmopolitan phytoplankton. *ISME J.* 9, 1365–1377. doi: 10.1038/ismej.2014.221
- von Dassow, P., van den Engh, G., Iglesias-Rodriguez, M. D., and Gittins, J. R. (2012). Calcification state of coccolithophores can be assessed by light scatter depolarization measurements with flow cytometry. *J. Plankton Res.* 34, 1011–1027. doi: 10.1093/plankt/fbs061
- Wang, X., Fu, F., Qu, P., Kling, J. D., Jiang, H., Gao, Y., et al. (2019). How will the key marine calcifier *Emiliana huxleyi* respond to a warmer and more thermally variable ocean? *Biogeosciences* 16, 4393–4409. doi: 10.5194/bg-16-4393-2019
- Willett, C. S. (2011). The nature of interactions that contribute to postzygotic reproductive isolation in hybrid copepods. *Genetica* 139, 575–588. doi: 10.1007/s10709-010-9525-1
- Winter, A., Henderiks, J., Beaufort, L., Rickaby, R. E. M., and Brown, C. W. (2014). Poleward expansion of the coccolithophore *Emiliana huxleyi*. *J. Plankton Res.* 36, 316–325. doi: 10.1093/plankt/fbt110
- Young, J., Geisen, M., Cros, L., Kleijne, A., Sprengel, C., Probert, I., et al. (2003). A guide to extant coccolithophore taxonomy. *J. Nanoplankton Res* 1, 1–132.
- Young, J. R., and Westbroek, P. (1991). Genotypic variation in the coccolithophorid species *Emiliana huxleyi*. *Mar. Micropaleontol.* 18, 5–23.
- Zhang, Y., Klapper, R., Lohbeck, K. T., Bach, L. T., Schulz, K. G., Reusch, T. B. H., et al. (2014). Between- and within-population variations in thermal reaction norms of the coccolithophore *Emiliana huxleyi*. *Limnol. Oceanogr.* 59, 1570–1580. doi: 10.4319/lo.2014.59.5.1570

**Conflict of Interest:** The authors declare that the research was conducted in the absence of any commercial or financial relationships that could be construed as a potential conflict of interest.

**Publisher's Note:** All claims expressed in this article are solely those of the authors and do not necessarily represent those of their affiliated organizations, or those of the publisher, the editors and the reviewers. Any product that may be evaluated in this article, or claim that may be made by its manufacturer, is not guaranteed or endorsed by the publisher.

Copyright © 2021 von Dassow, Muñoz Farias, Pinon, Velasco-Senovilla and Anguita-Salinas. This is an open-access article distributed under the terms of the Creative Commons Attribution License (CC BY). The use, distribution or reproduction in other forums is permitted, provided the original author(s) and the copyright owner(s) are credited and that the original publication in this journal is cited, in accordance with accepted academic practice. No use, distribution or reproduction is permitted which does not comply with these terms.